Novel SACX Solders with Drop Test Performance Outperforming Eutectic Tin-Lead

Dr. Weiping Liu and Dr. Ning-Cheng Lee
Indium Corporation of America

ABSTRACT
A family of SACX alloys has been developed with significant improvement in drop test performance on NiAu surface finish. Dopants such as Mn, Bi, Ti, Ce, and to a less extent Y for SAC105 have been observed to show very positive effect when used alone or in combination, with Mn exhibiting the most profound effect. SAC+Mn outperformed not only SAC alloys, but also Sn63, thus completely altered the shaky position of SAC systems caused by fragility of solder joints. The melting and intermetallic formation properties are not affected by the dopants. Mn tends to migrate toward IMC and accumulate near IMC layer in the form of $MnSn_2$ particles. Thermal aging results in further improvement of drop test performance.

Key words: lead-free, SnAgCu, SAC, solder, drop test, fragility, reliability.

INTRODUCTION

Due to the RoHS requirement, lead is to be removed from solder materials used in electronic industry. Among a variety of lead-free solder alternatives, SnAgCu alloys are the most popular choices. This is mainly due to their superior performance in physical, mechanical, and fatigue properties as well as their reasonable soldering behavior and cost. However, adoption of these alloys has been hampered by the fragility of solder joints, as reflected by their poor drop test performance relative to 63Sn37Pb. This is particularly an issue for portable devices employing area array packages such as BGAs and CSPs [1-7]. Although reduction of Ag content in SnAgCu alloys has been found to be helpful [8], the performance is still inferior to that of eutectic tin-lead. In this work, a family of SnAgCu alloys modified with small amount of additives was developed and studied, with results discussed below.

EXPERIMENTAL

1. Alloys

The majority of solder alloys studied is by introducing a small amount of one or two additional elemental dopants to 98.5Sn1Ag0.5Cu (SAC105), and is generally represented as SACX. In some cases, the content of Ag and Cu are also altered. 63Sn37Pb (Sn63), 95.5Sn3.8Ag0.7Cu (SAC387), and SAC105 are used as control.

2. Tests

2.1 Melting Behavior

The melting behavior of solder alloys was studied with Differential Scanning Calorimetry (DSC). The sample size was around 5-15 mg, and scanning rate 10°C/min. For each alloy, the sample was scanned twice. The sample was first scanned from ambient temperature up to 350°C, followed by cooling down to ambient temperature naturally, then scanned again up to 350°C. The second scanning thermograph was used to represent the melting behavior of alloys.

2.2 Drop Test

The drop test was conducted by a procedure described below. The sample was a simulated BGA assembly. The BGA coupon is 40 mm x 40 mm, with 3 x 3 array distributed electroplated Ni/Au pads (2 mm diameter), as shown in Figure 1. The PCB test board is 80 mm x 80 mm, with 4 drilled holes (6 mm diameter) at the corners for mounting onto steel block with bolts. The surface finish of the corresponding pads (2 mm diameter) on PCB is also electroplated Ni/Au.

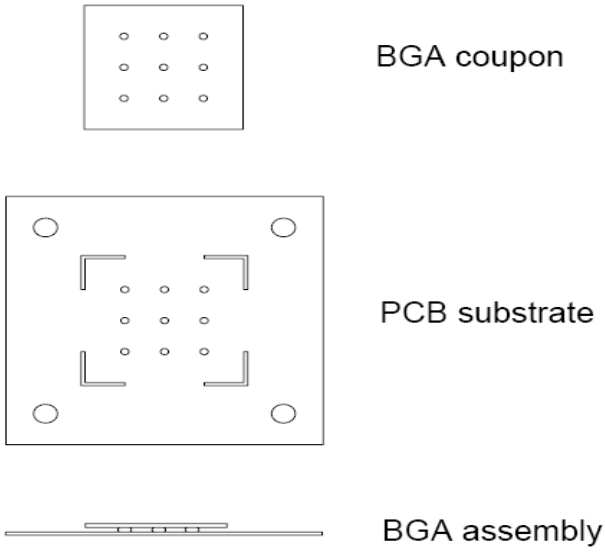

Figure 1 - Schematic of test coupons and simulated BGA assembly.

To produce a simulated BGA component, the solder spheres of a given alloy were first mounted onto PCB substrate with the use of a no-clean flux and profile A with a peak temperature 240°C. This bumped PCB was then mounted with BGA coupon preprinted with the same no-clean flux on pads and reflowed with profile A. The simulated BGA assembly was evaluated for drop test as-reflowed and after aging at 150°C for 4 weeks. The BGA assembly was mounted onto the steel block of drop testing equipment, as shown in Figure 2. The height used for drop test is 0.5 meter. For each test condition, 10 simulated BGA assemblies were used.

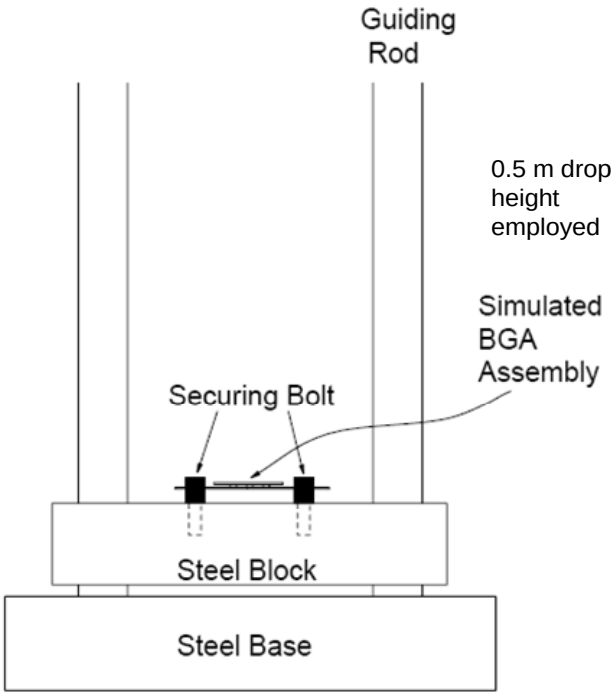

Figure 2 - Schematic of drop tester setup. The clearance between PCB and steel block is 5 mm.

2.3. Microstructure

The fracture surfaces and cross-sections of drop test samples were examined for microstructure with optical microscope and SEM/EDS. In some cases, elemental mapping was conducted on the cross-sectioned samples.

2.4. Creep Test

A dumbbell shaped solder specimen was used for creep test. The stress range was explored for a measurable steady strain rate at room temperature. The steady strain rate of at least two different stresses was determined for each alloy.

RESULTS

1. Melting Behavior

Addition of small amount of additives appears to have negligible effect on the melting behavior of SAC alloys. Table 1 exemplifies the melting temperature of some solder alloys determined at the second scan of DSC analysis. Figure 3 shows the DSC thermographs of second scan for Sn63, SAC305, SAC105, and Sn1.1Ag0.64Cu0.13Mn (SAC0.13Mn).

Table 1 - Melting behavior of solder alloys at the second scan of DSC analysis.

Alloys	Solidus (°C)	Liquidus (°C)
Sn1.1Ag0.64Cu0.13Mn	217.52	227.26
Sn1.13Ag0.6Cu0.16Mn	217.81	225.98
Sn1.07Ag0.58Cu0.037Ce	217.65	226.14
Sn1.0Ag0.46Cu0.3Bi0.1Mn	216.22	226.98
Sn1.05Ag0.73Cu0.067Ti	217.59	227.56
SAC105	217.18	226.8
SAC305	217.64	222.81
Sn63	180.75	183.72

2. Drop Test

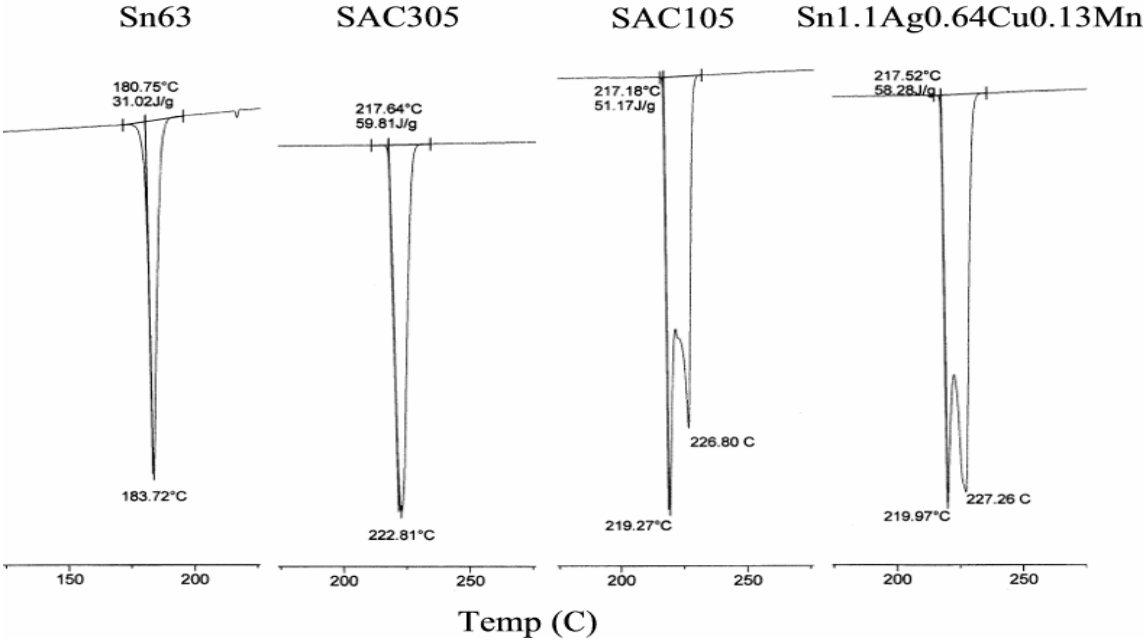

Figure 3 - DSC thermographs of second scan for Sn63, SAC305, SAC105, and Sn1.1Ag0.64Cu0.13Mn.

The drop test results of as-reflowed samples are shown in Figure 4. SAC387 and SAC305 survived in average only 1.1 and 1.2 drops respectively before failure. SAC105 exhibits a mean drop number of 5.1, hence is considerably better than SAC387 and SAC305. This is consistent with work of Date et al. [8]. However, compared with Sn63, with a mean drop number 23.8, SAC105 is still significantly inferior.

The effect of dopants depends heavily on the dopant chemistry. Ni and Ge cause adverse effect on SAC105, exhibiting a mean value of 1.4 and 1.2, respectively. Y is insignificant. Ti, with a mean value of 10.6, exhibits a moderately positive effect on drop test. The effect of Ce is interesting, with test results showing a mean value of 20.9 and 3.5 for SAC105 with 0.037Ce and 0.12Ce, respectively. This high sensitivity of SAC alloy toward Ce dopant level is repeatable in another

confirmation run of tests. Bi, with a mean value of 14.6, and Mn displayed a positive effect. In the case of Mn, the impact is fairly sensitive to the content of Mn. The drop test performance improves with increasing Mn content, reaching a maximum mean value of 35.4 at 0.13Mn content, then decreases with further increase in Mn content. Addition of more than one elemental dopant does not bring in synergistic effect, as demonstrated by SAC105+BiMn and SAC105+BiY systems. SAC105+0.2Mn0.02Ce showed a mean value of 28.5, higher than both 0.16Mn and 0.25Mn cases. Due to the large standard deviation of test, the actual effect of dual dopants needs to be further clarified.

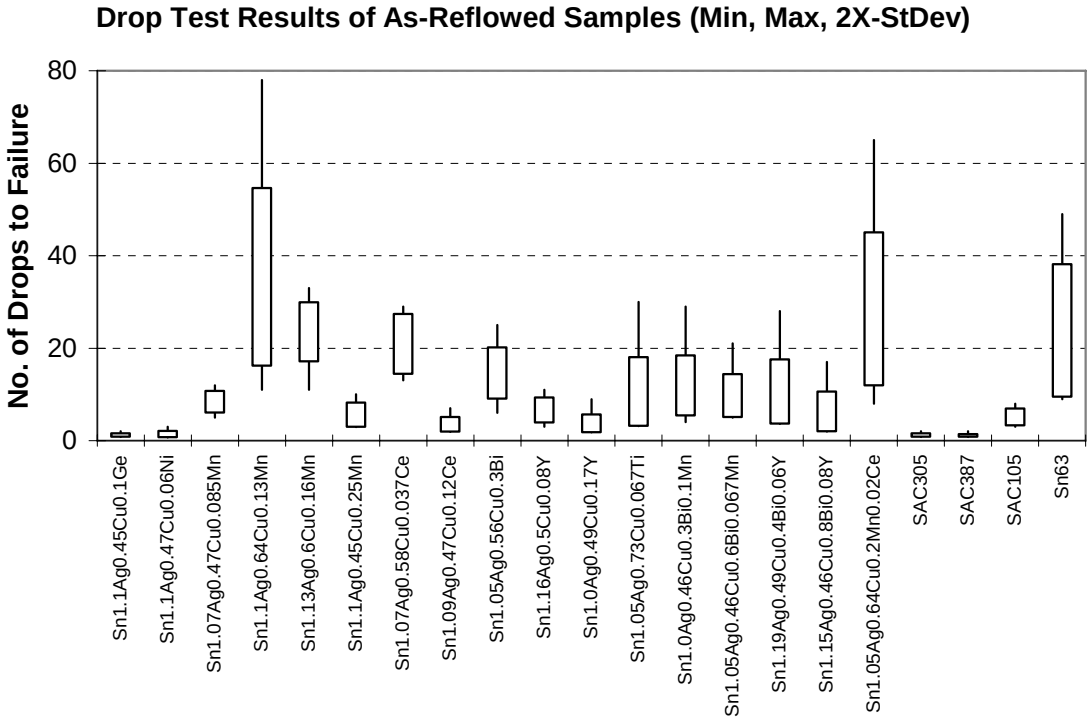

Figure 4 - Drop test results of as-reflowed samples. The thin line represents minimum and maximum values; the box represents two standard deviations, with mid point being the mean value.

The drop test performance was also studied for samples thermally aged at 150°C for 4 weeks, with results shown in Figure 5. Comparing the data of as-reflowed versus thermally aged, as shown in Figure 6, it is interesting to note that while the mean value of Sn63 deteriorates significantly down to 4.0, many SACX alloys exhibit a higher drop test mean value after aging. Considering both as-reflowed and aged data, Sn1.1Ag0.64Cu0.13Mn SAC0.13Mn), Sn1.13Ag0.6Cu0.16Mn (SAC0.16Mn), and Sn1.07Ag0.58Cu0.037Ce are the most promising in drop test performance.

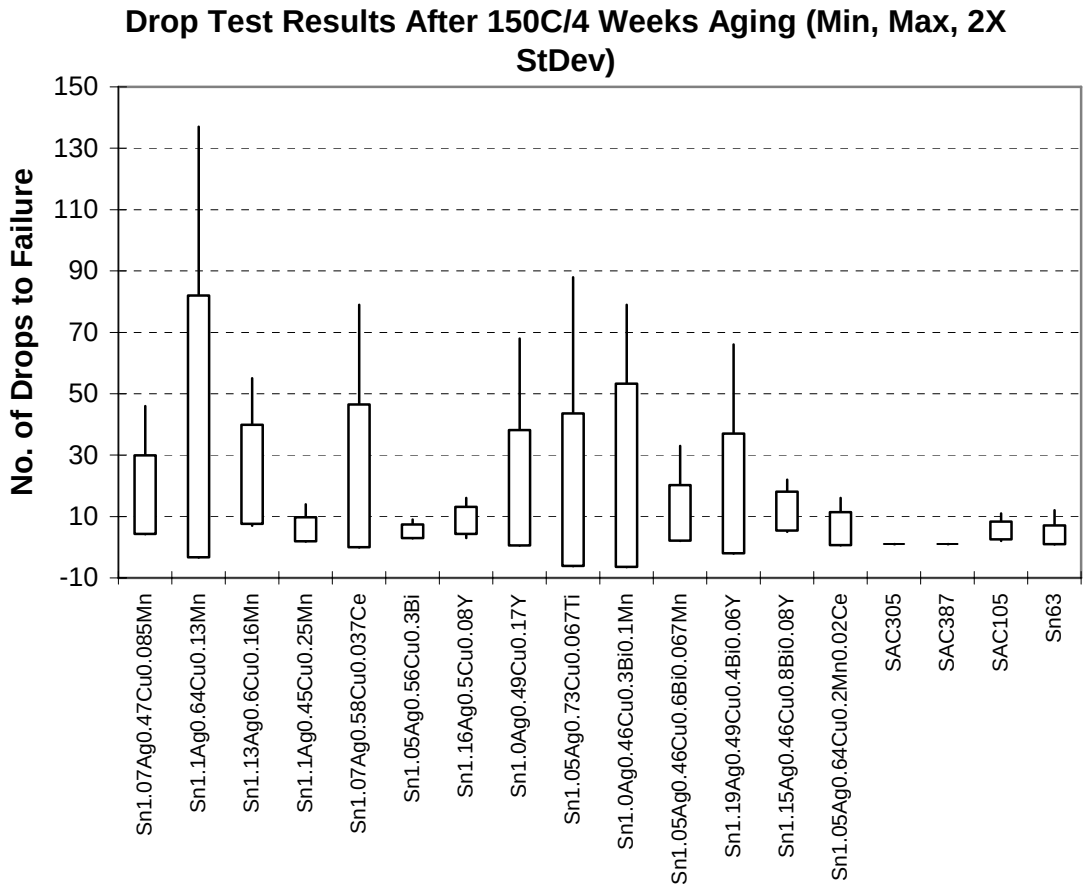

Figure 5 - Drop test results of samples after thermally aged at 150°C for 4 weeks. The thin line represents minimum and maximum values,

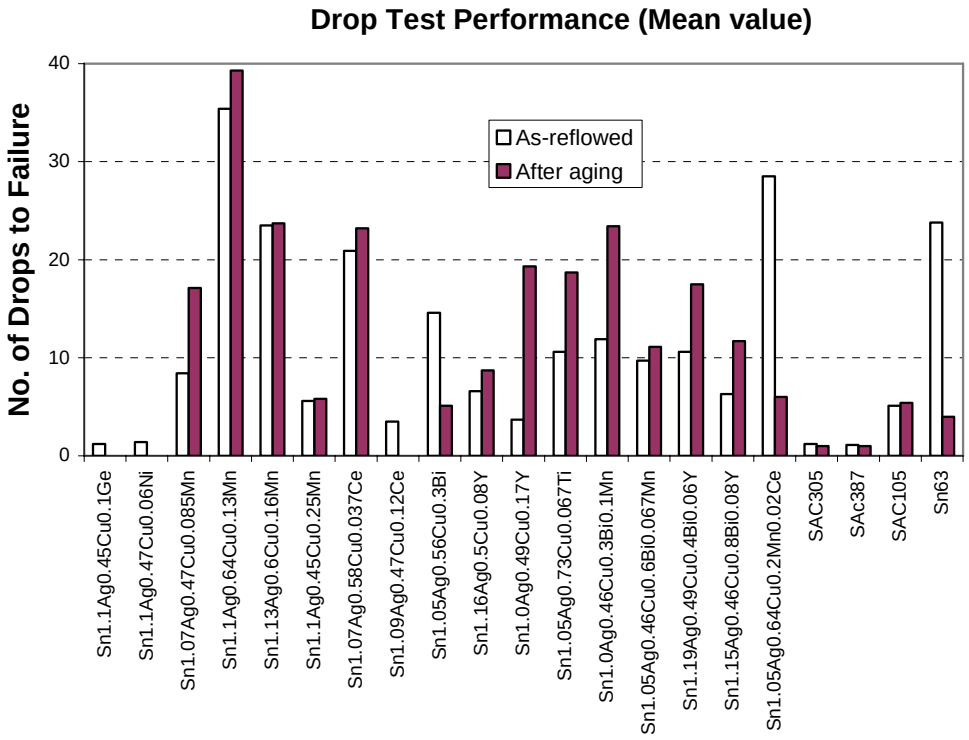

Figure 6 Mean values of drop test results for as-reflowed and after aging samples.

The effect of Mn dopant on SAC alloys with various Ag content was also investigated for as-reflowed samples, with results

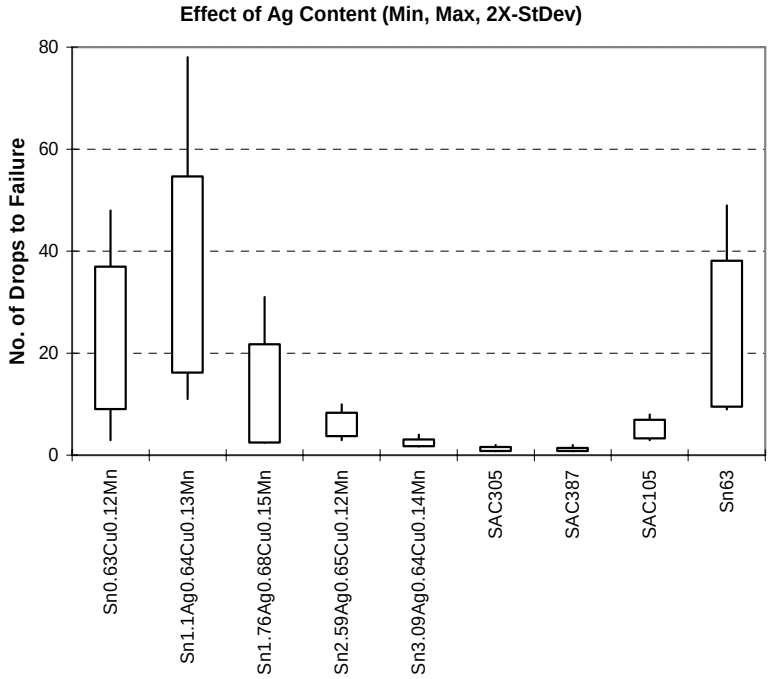

Figure 7 - Effect of Ag content on drop test performance for as-reflowed samples.

shown in Figure 7. At about 0.13% Mn content, the mean value of drop test was 23, 35.4, 12.1, 6.0, and 2.4 for SACX alloys

with Ag content 0, 1.1, 1.8, 2.6, and 3.1%, respectively. Except for 3.1%Ag sample, all other samples with a lower Ag content exhibit a mean value greater than that of SAC105 (mean value 5.1), not to mention SAC305 (mean value 1.20) and SAC387 (mean value 1.1). Although a lower Ag content generally results in a better drop test performance for SAC alloy system [8], use of Mn dopant essentially elevates the drop test performance of 2.6Ag alloy to that of SAC105.

3. Microstructure
3.1 Fracture Site Identification
3.1.1 SAC0.13Mn

The fracture location of drop test specimen is a function of material properties. Figure 8 shows fracture of SAC0.13Mn involving near-interface rupture and through the bulk solder. Figure 9 shows a fractured joint of SAC0.13Mn occurring primarily at interface between solder and pad. A close-up look at the center of the pad shown in Figure 9 suggests it is composed of intermetallics, as shown in Figure 10. The exact location of fracture is further elucidated by examining the cross-sectioned samples. Figure 11 shows the cross-section of solder joint of SAC0.13Mn and Figure 12 shows SEM image of cross-section of fracture surface at solder side of a drop test sample of SAC0.13Mn. The intermetallic layer on top of solder indicates that the intermetallic layer mainly remains on solder side. Therefore, by examining both Figure 10 and Figure 12, it can be deduced that the fracture occurred within intermetallic layer, and is very close to the Ni layer. This stipulation is supported by the EDX of pad center of fracture surface of drop test sample of SAC0.13Mn, as shown in Figure 13, where large amount of Sn, besides some Cu, is found on the pad surface.

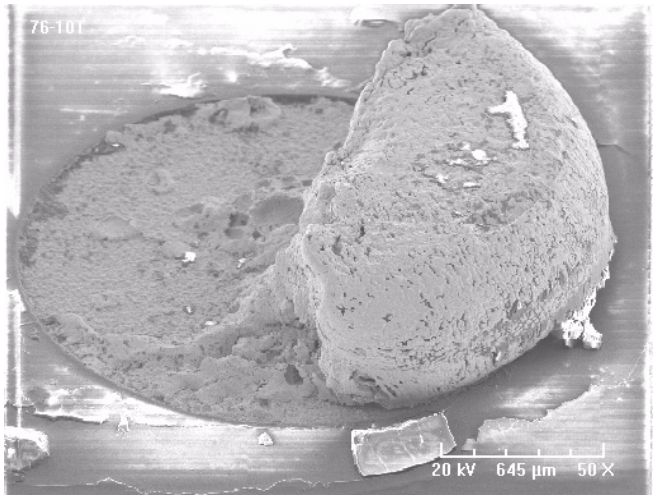

Figure 8 - 50X SEM image of fracture surface of drop test sample of SAC0.13Mn solder joint.

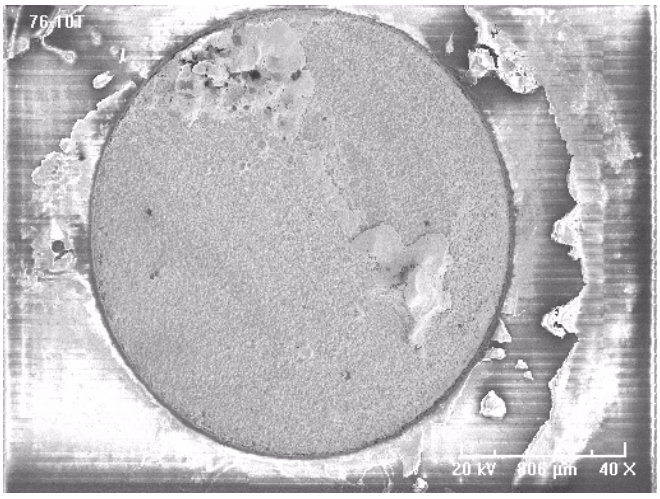

Figure 9 - 40X SEM image of fracture surface of drop test sample of SAC0.13Mn.

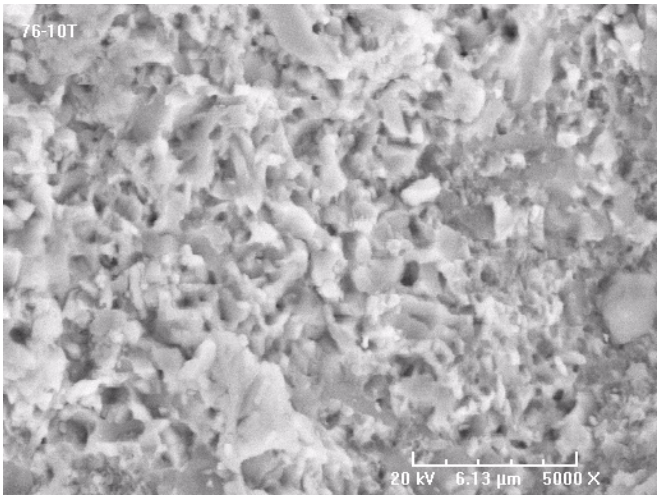

Figure 10 - 5000X SEM image of near center of pad of fracture surface of drop test sample of SAC0.13Mn.

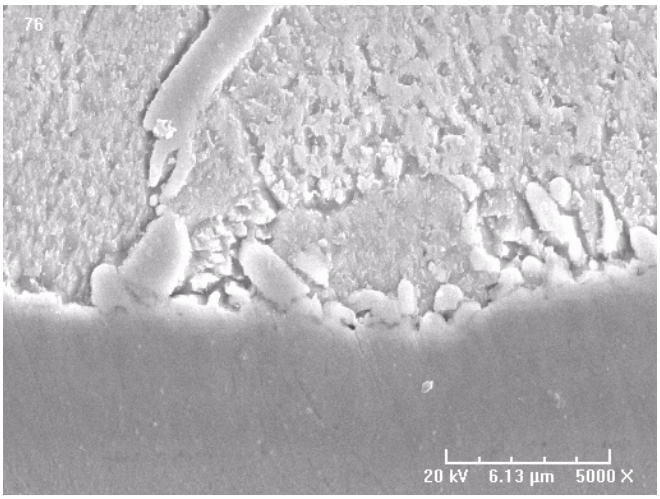

Figure 11 - 5000X SEM image of cross-section of solder joint interface of drop test sample of SAC0.13Mn.

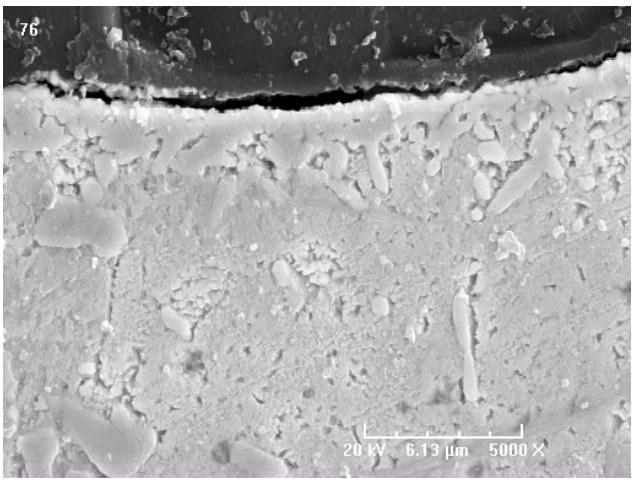

Figure 12 - 5000X SEM image of cross-section of fracture surface at solder side of drop test sample of SAC0.13Mn, showing most of the intermetallic layer remain on solder side.

3.1.2 SAC105, SAC305, and Sn63

The occurrence of fracture around the interface of intermetallics and Ni layer is also observed for SAC105 and SAC305. Figure 14 shows SEM images (8000X) of cross-section (top) and fractured surface on solder side (bottom) for SAC105 solder, while Figure 15 shows SEM images (8000X) of cross-section (top) and fractured surface on solder side (bottom) for SAC305 solder. Sn63 behaves somewhat different from SAC alloys. Figure 16 shows SEM images (2000X) of cross-section (top) and fractured surface on solder side (bottom) for Sn63 solder. Although fracture still occurred around the interface of intermetallics and Ni layer, more solder remains on the pad, as shown in Figure 17.

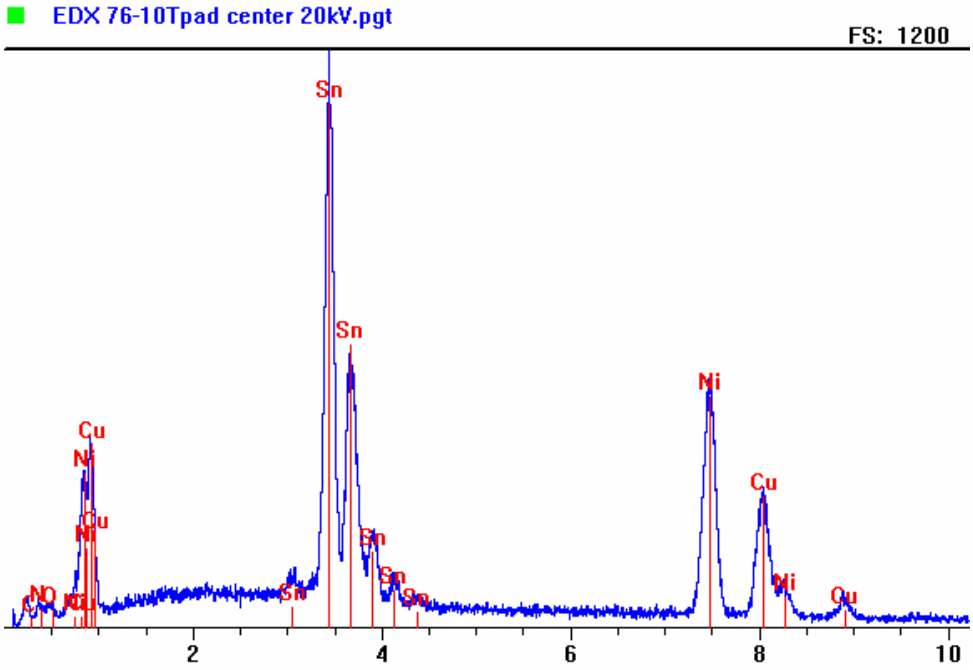

Figure 13 - EDX of pad center of fracture surface of drop test sample of SAC0.13Mn. Besides Ni, presence of Cu and large amount of Sn is observed.

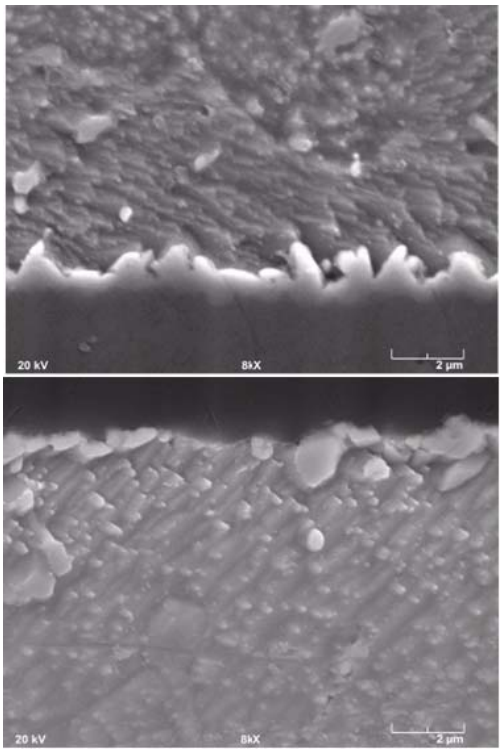

Figure 14 - SEM images (8000X) of cross-section (top) and fractured surface on solder side (bottom) for SAC105 solder joint.

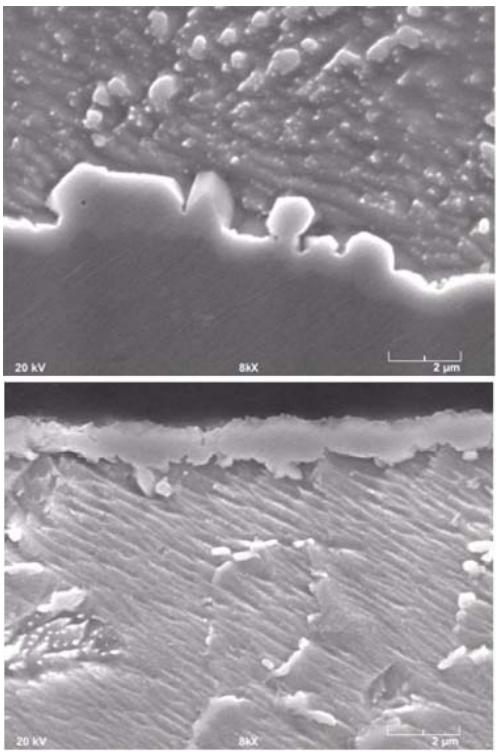

Figure 15 - SEM images (8000X) of cross-section (top) and fractured surface on solder side (bottom) for SAC305 solder joint.

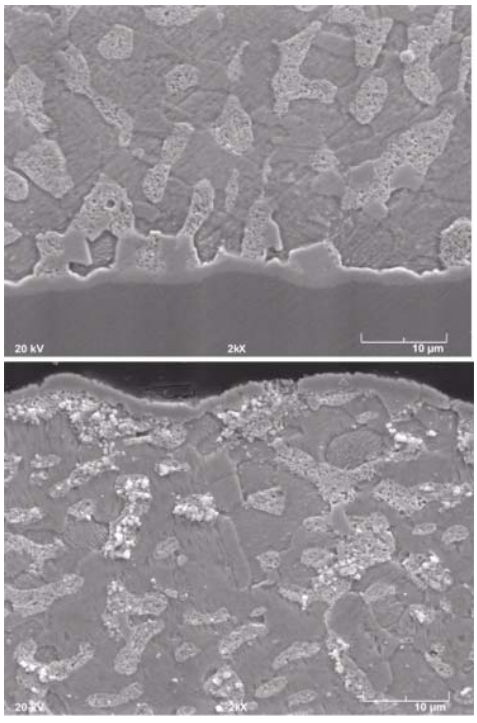

Figure 16 - SEM images (2000X) of cross-section (top) and fractured surface on solder side (bottom) for Sn63 solder joint.

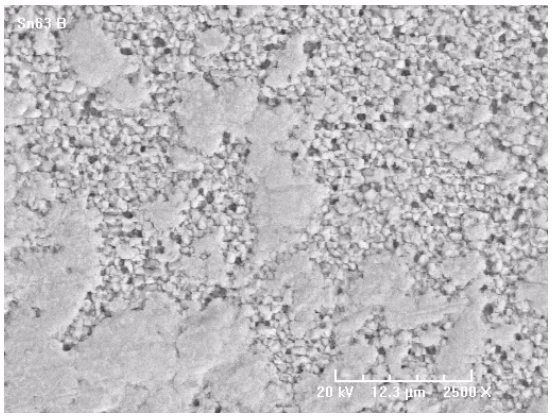

Figure 17 - 500X (top) and 2500X (bottom) SEM images of fracture surface of pad side of drop test sample of Sn63.

3.1.3 Fracture Pattern

The fracture pattern of alloys was investigated by examining the location of fracture site. All fracture surfaces were classified as one of the three fracture modes: (1) fracture at interface between solder and pad, (2) fracture within solder, and (3) a mixed mode of interface and solder. Figure 18 shows the fracture pattern distribution of Sn63, SAC305, SAC105, and SAC0.13Mn for as-reflowed drop test samples. The drop test performance, as shown in Figure 4, in general improves with increasing percentage of mixed mode and solder mode. This relation reflects that a tougher interface is crucial for a better drop test performance. However, this relation is not applicable when comparing Sn63 with SAC0.13Mn.

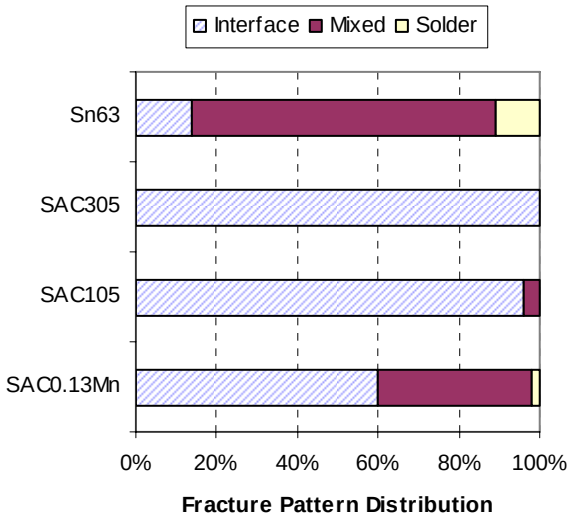

Figure 18 Effect of alloy on fracture pattern for as-reflowed drop test samples.

3.2 Ring

For alloys with poor drop test performance, the fracture surface typically is flat, as exemplified by Figure 19 for SAC305. However, alloys with high drop test performance often exhibit ring pattern, as exemplified by Figure 20 for Sn1.1Ag0.45Cu0.25Mn and Sn63, and Figure 21 for Sn1.13Ag0.6Cu0.16Mn. A close-up look at the ring shows ridge formation (see Figure 21). The pads with ring pattern often show a convex profile. This is verified by examining the cross-section of those pads, as exemplified by Figure 22 for Sn1.05Ag0.56Cu0.3Bi. In Figure 22, the convex shape of pad can be seen clearly, and is accompanied by a crack in the laminate layer underneath the pad. It appears that, upon drop test, the multiple bouncing of solder joint repeatedly lifted the pad, and the ring serves as water mark for the incremental fracture of solder joint.

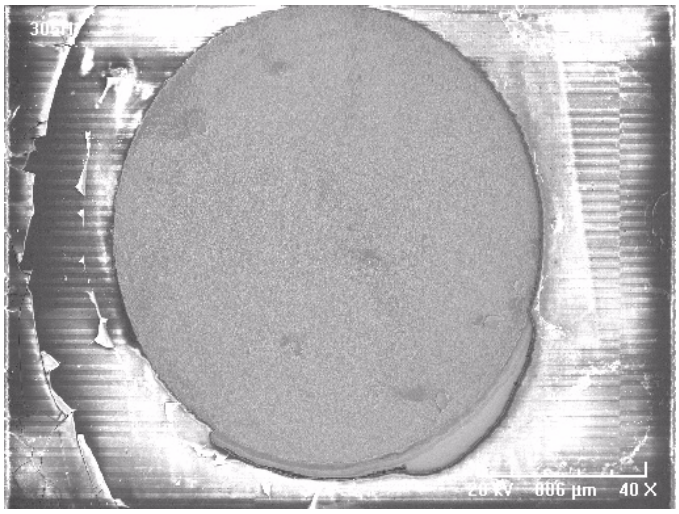

Figure 19 - Fracture surface of drop test sample of SAC305.

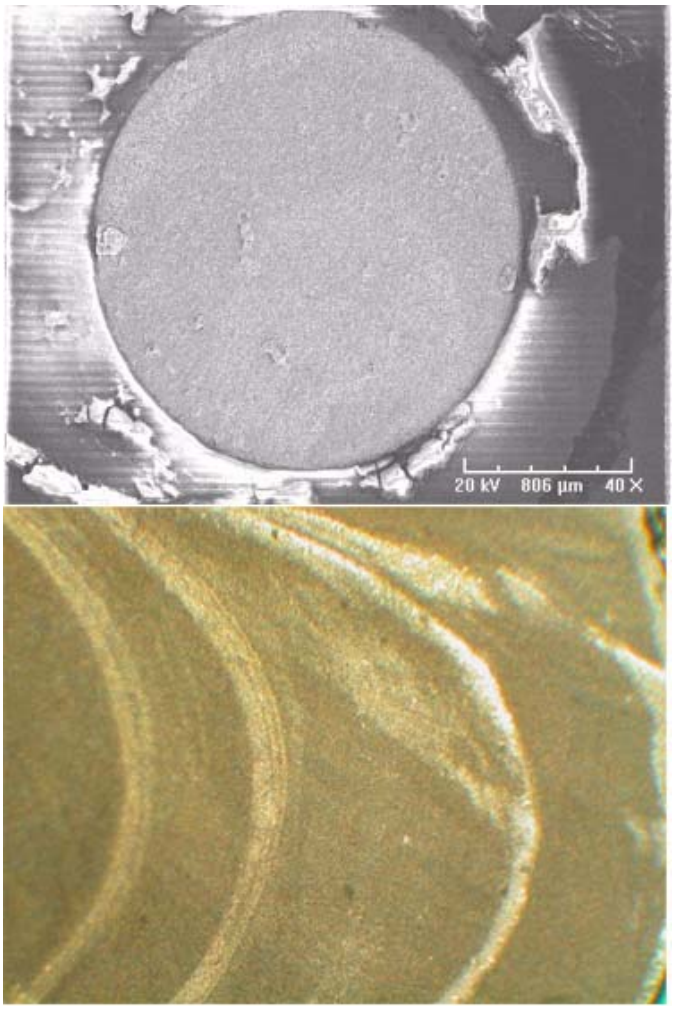

Figure 20 - SEM image (left) of fracture surface of drop test sample of Sn1.1Ag0.45Cu0.25Mn and photo of fracture surface of Sn63 sample (right).

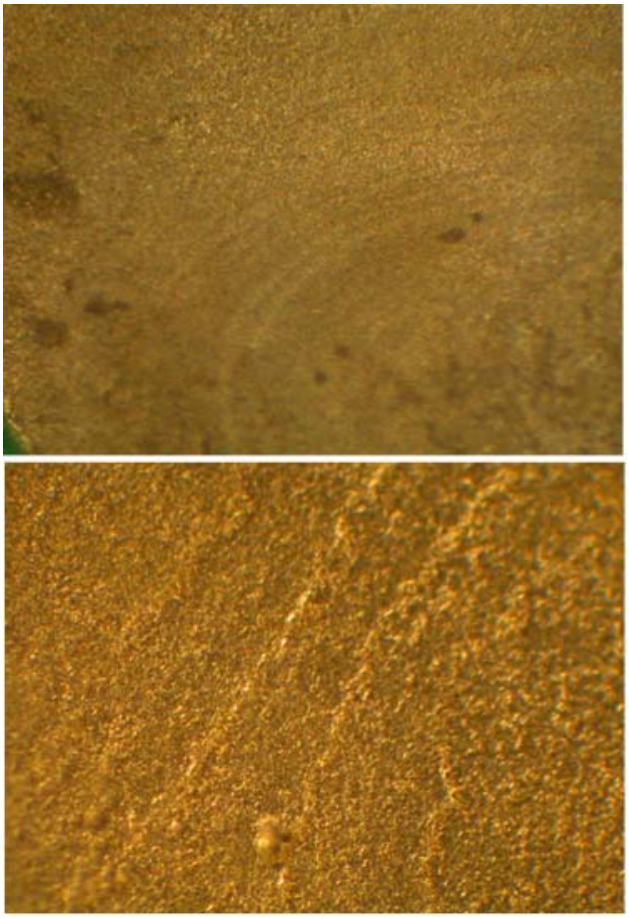

Figure 21 - Ring pattern (top) on pads of drop test sample of Sn1.13Ag0.6Cu0.16Mn and close-up look (bottom) of the ring.

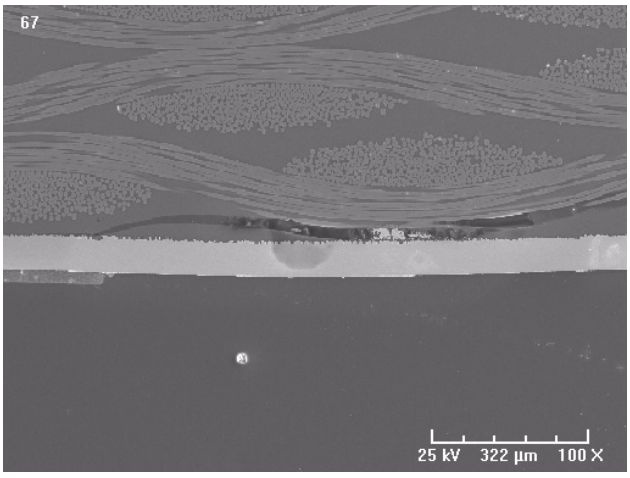

Figure 22 - SEM image (100X) of cross-section of pads with ring pattern for fractured drop test sample of Sn1.05Ag0.56Cu0.3Bi.

3.3 Element Mapping

In order to investigate the role of Mn in drop test performance, EDX elemental mapping on fractured drop test sample of SAC0.13Mn is conducted. Figure 23 shows mapping for open end of solder portion fractured at PCB pad side for drop test sample of SAC0.13Mn, while Figure 24 shows mapping for middle section of solder fractured at interface with PCB for drop test sample of SAC0.13Mn. Although the intensity of Mn is weak due to its low concentration, Mn is observed to cluster near

intermetallics layer, as seen in Figure 23. At location farther way from the intermetallics layer, such as the middle region of solder joint (see Figure 24), no Mn can be discerned. Furthermore, negligible amount of Mn can be detected near the BGA pad side.

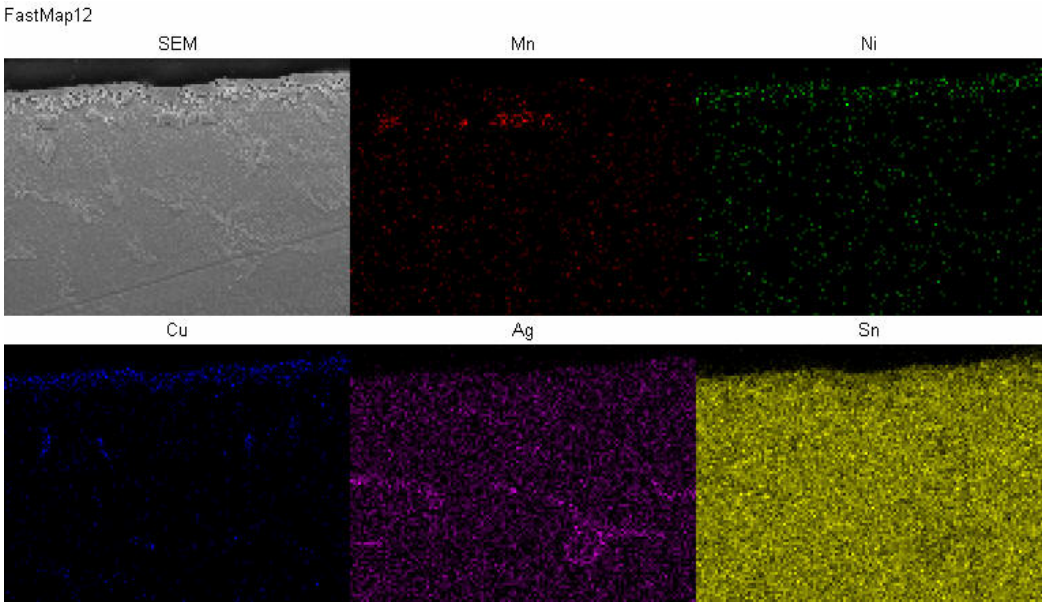

Figure 23 - Elemental mapping (2000X) for open end of solder portion fractured at PCB pad side for drop test sample of SAC0.13Mn.

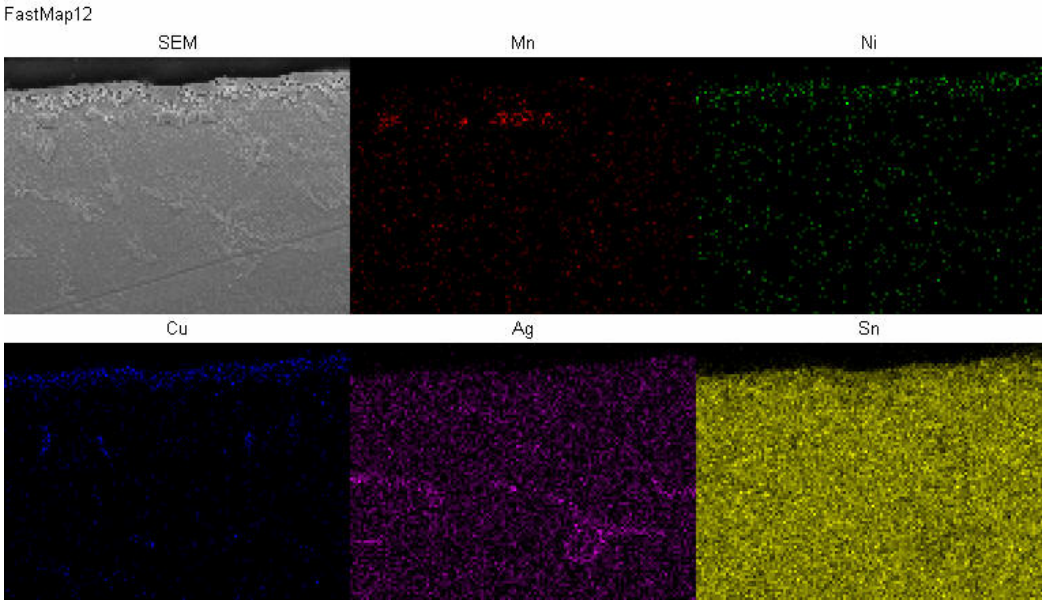

Figure 23 - Elemental mapping (2000X) for open end of solder portion fractured at PCB pad side for drop test sample of SAC0.13Mn.

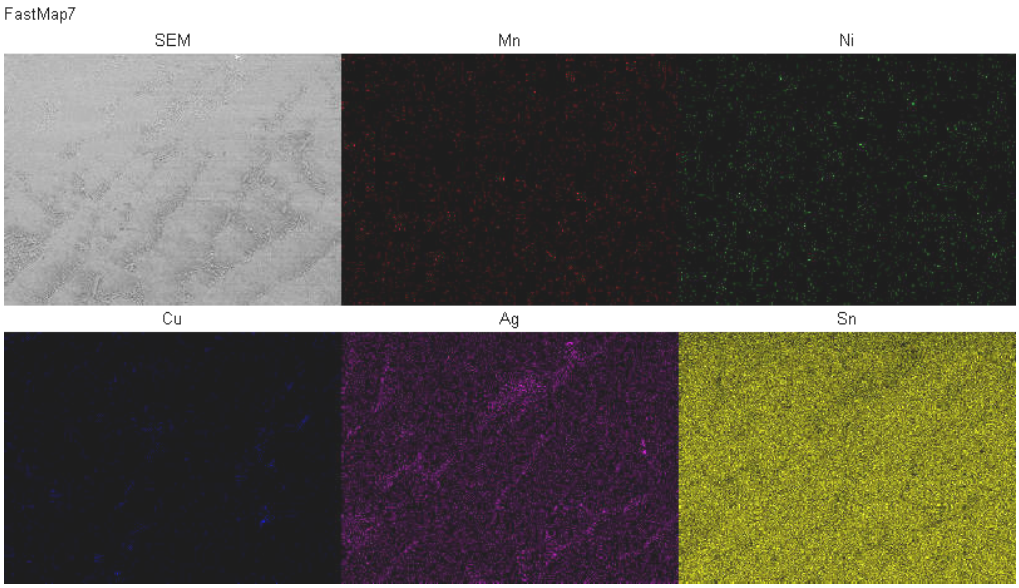

Figure 24 - Elemental mapping (800X) for middle section of solder fractured at interface with PCB for drop test sample of SAC0.13Mn.

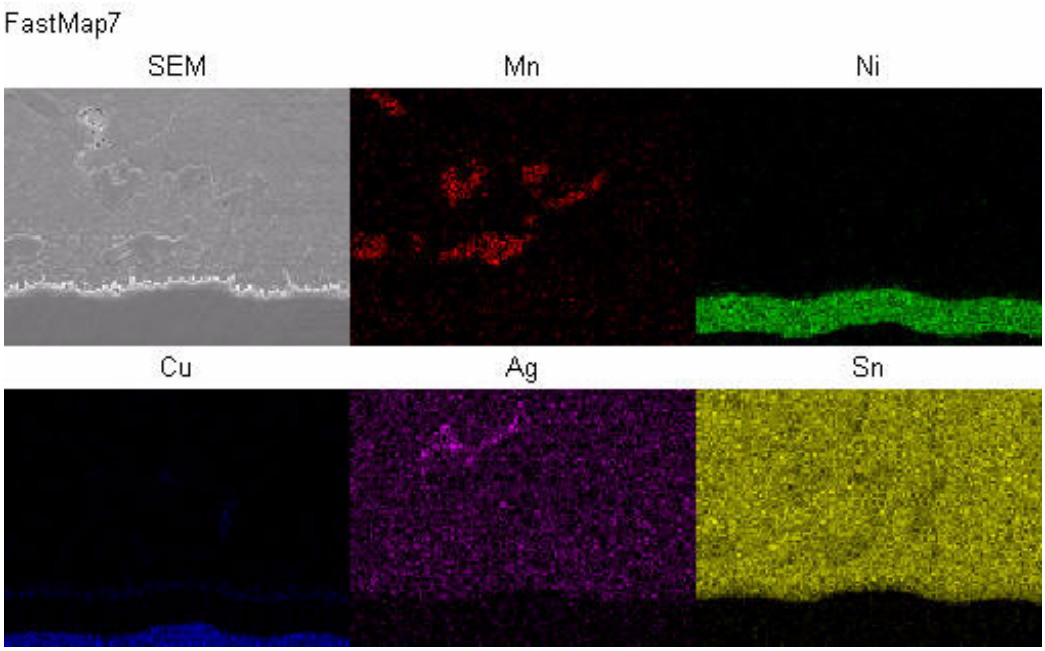

Figure 25 - EDX elemental mapping (2000X) for drop test sample of SAC0.25Mn at interface of solder joint.

In this study, the solder bump was formed on PCB first, then followed by BGA coupon attachment. Mn appears to migrate toward PCB side during the first reflow, and scattered near the intermetallics layer. At the second reflow for BGA coupon attachment, the Mn seems to be unable to migrate back toward the BGA end in time to form an equilibrated distribution at both ends of solder joint.

The form of Mn present in solder joint was studied by examining Sn1.1Ag0.45Cu0.25Mn (SAC0.25Mn), which exhibits a higher concentration of Mn than SAC0.13Mn, thus a greater sensitivity in analysis. Figure 25 shows EDX elemental mapping for drop test sample of SAC0.25Mn at interface of solder joint. The location of Mn is observed to be coincident with particulates, which are identified as $MnSn_2$ intermetallics.

4. Intermetallics

The role of intermetallic thickness and growth rate in drop test performance was studied, with results shown in Table 2. All alloys except SAC387 exhibit an intermetallic compound (IMC) thickness around 0.9 μm for as-reflowed joints. This thickness roughly doubled after aging at 150°C for 4 weeks. By comparing Figure 6 with Table 2, no correlation can be established between intermetallics thickness, intermetallics growth rate, and drop test performance.

Table 2 - Relation between solder alloys and intermetallic compound thickness for as-reflowed and thermally aged condition.

Solder alloys	IMC (μm) As-reflowed	IMC (μm) Aged @150°C for 4 weeks
SAC0.13Mn	0.93	1.85
SAC0.16Mn	0.95	1.72
Sn63	0.86	2.04
SAC305	1.05	1.83
SAC387	1.4	2.5
SAC105	0.94	1.56

5. Hardness

The effect of bulk hardness of solder alloy on drop test performance was also investigated. The Vicker Hardness was determined for several representative alloys, with results shown in Table 3. Although the drop test performance appears to improve with decreasing hardness, this perceived relation suffers significant data scattering, suggesting the bulk solder hardness is not a dictating factor.

6. Creep Behavior

The room temperature creep properties of the lead-free alloys were studied, with results shown in Figure 26. Majority of the SAC(X) alloys, including SAC0.13Mn, exhibit a lower creep rate than Sn63 at low stress condition. However, their creep rate increases rapidly with increasing stress, and at high stress condition, most of the SAC(X) show a higher creep rate. A lower creep rate often suggests a longer fatigue life. In other words, at low stress condition, many of the SACX alloys not only exhibit a drop test performance better than SAC alloys or even better than Sn63, but very likely also exhibit a fatigue life better than Sn63.

DISCUSSION

1. Surface Finish

The surface finish employed in this study is electroplated NiAu. For other surface finishes such as OSP or immersion Ag, the performance should be checked also.

Table 3 - Hardness of solder alloys for as-reflowed and aged at 150°C for 4 weeks.

Alloy Composition	Hv (VHN) as-reflowed	Hv (VHN) aged
Sn1.13Ag0.6Cu0.16Mn	12.6	--
Sn1.1Ag0.45Cu0.25Mn	12.9	13.2
Sn1.07Ag0.58Cu0.037Ce	13.1	--
Sn1.05Ag0.56Cu0.3Bi	14.6	--
Sn1.05Ag0.73Cu0.067Ti	13.2	--
SAC387	15.9	15.2
SAC105	12.9	12.8
Sn63	12.5	--

2. Mn

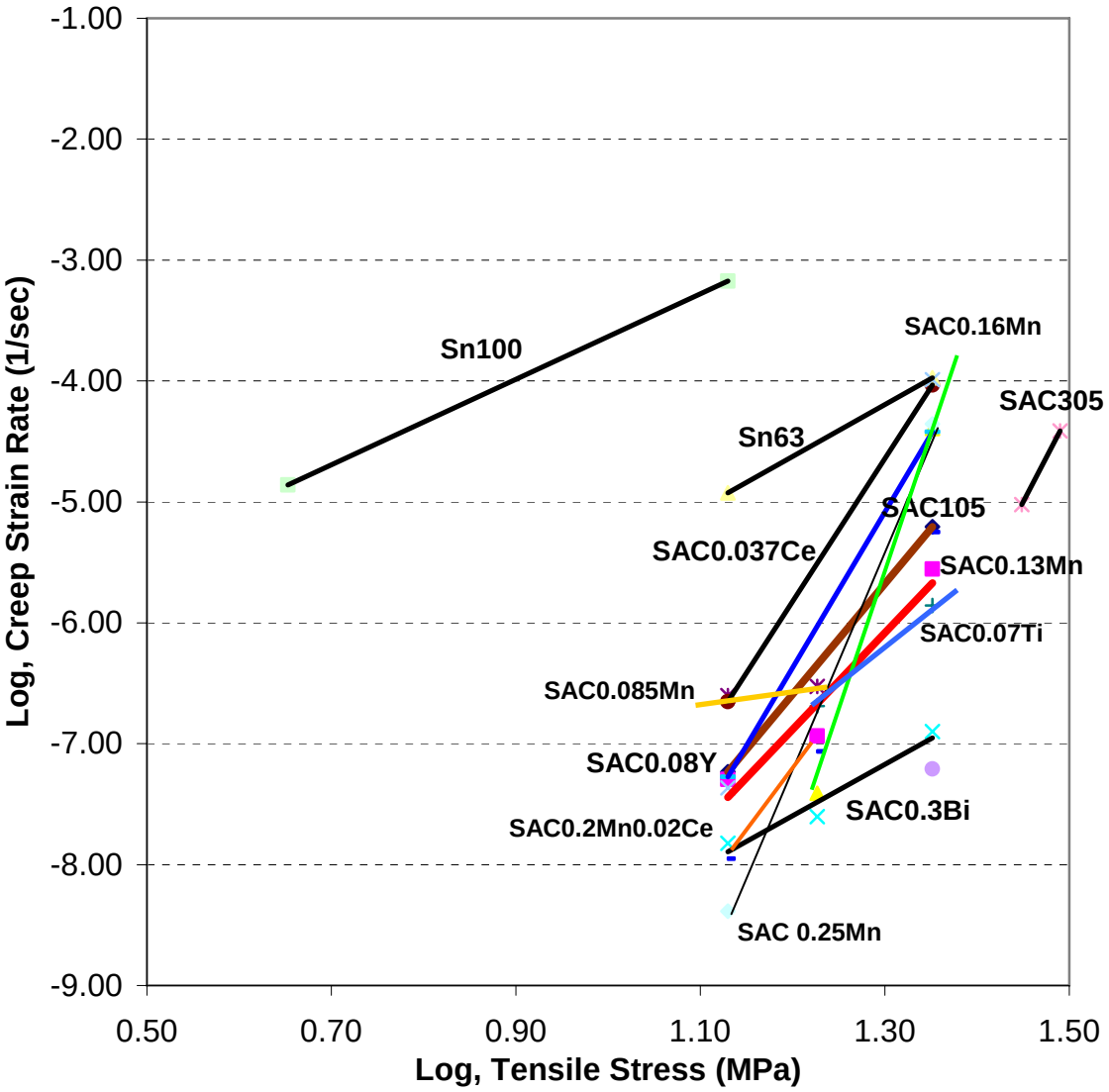

Figure 26 - Creep test results of solder alloys determined at room temperature

The exact role of Mn in enhancing the drop test performance is still not well understood yet. But, there are several clues for its possible role. First, Mn is not found in IMC layer, and the IMC thickness and IMC growth rate are not affected. Second, $MnSn_2$ particles tend to accumulate near IMC layer. Third, the bulk hardness of SAC is not altered by the addition of Mn dopant. Fourth, the fracture mode shifted from interface toward solder fracture, suggesting stronger bond strength between IMC and Ni layer. Since IMC layer is not altered in either chemical structure or thickness or growth rate, this stronger bond strength presumably is caused by a reduced stress from solder exerted onto IMC layer. This is similar in mechanism to the effect of reducing Ag content. As to why the $MnSn_2$ will result in a reduced stress is not clear at this stage.

However, since Mn tends to migrate and accumulate near the IMC layer of the first soldering pad, such as at BGA bumping stage, the other end of the solder joint, such as at BGA assembly stage, may not benefit equally from the use of Mn. To provide Mn source for the second soldering process at SMT assembly stage in order to maximize the performance on drop test, use of SAC+Mn solder paste would be a recommended solution.

3. Improved Drop Test Performance with Aging

In general, the SACX alloys exhibit a better performance with thermal aging. This could be attributed to softening of SACX solder due to consolidation of IMC particles during aging. On the other hand, it may also be due to further migration of dopants toward IMC layer.

CONCLUSION

A family of SACX alloys has been developed with significant improvement in drop test performance on NiAu surface finish. Dopants such as Mn, Bi, Ti, Ce, and to a less extent Y for SAC105 have been observed to show very positive effect when used alone or in combination, with Mn exhibiting the most profound effect. SAC+Mn outperformed not only SAC alloys, but also Sn63, thus completely altered the shaky position of SAC systems caused by fragility of solder joints. The melting and intermetallic formation properties are not affected by the dopants. Mn tends to migrate toward IMC and accumulate near IMC layer in the form of $MnSn_2$ particles. Thermal aging results in further improvement of drop test performance.

[Patent pending for novel alloys presented in this paper]

ACKNOWLEDGEMENT

The authors are grateful for the great assistance provided by Paul Bachorik on many of the testing involved in this work.

REFERENCE

1. C. Chiu, K. Zeng, R. Stierman, D. Edwards, and K. Ano, "Effect of Thermal Aging on Board Level Drop Reliability for Pb-free BGA Packages", ECTC, p.1256. June, 2004.
2. D. Henderson, "On the question of SAC solder alloy – Cu pad solder joint fragility", Webcast Meeting on SAC Solder Joint Fragility, Binghamton, NY, September, 2004
3. S. K. Saha, S. Mathew and S. Canumalla, "Effect of Intermetallic Phases on Performance in a Mechanical Drop Environment: 96.5Sn3.5Ag Solder on Cu and Ni/Au Pad Finishes", ECTC, S29p5, June, 2004.
4. M. Amagai, Y. Toyoda, T. Ohnishi, S. Akita, "High Drop Test Reliability: Lead-free Solders", ECTC, S29p7, June 2004.
5. T. Gregorich and P. Holmes, J. Lee, C. Lee, "SnNi and SnNiCu Intermetallic Compounds Found When Using SnAgCu Solders", IPC/Soldertec Global 2nd International Conference on Lead Free Electronics, Amsterdam, Netherland, June 23, 2004.
6. M. Date, T. Shoji, M. Fujiyoshi, K. Sato, and K. N. Tu, "Impact Reliability of Solder Joints", ECTC, June, 2004.
7. P.A. Kondos & S. Mandke, "Kirkendall voiding in Cu pads and other pad issues", UIC Fragile SAC Joint Meeting. Binghamton, NY, Oct. 7, 2004.
8. M. Date, T. Shoji, M. Fujiyoshi, and K. Sato, "Pb-free Solder Ball with Higher Impact Reliability", Intel Pb-free Technology Forum, July 18-20, 2005, Penang, Malaysia.

Novel SACX Solders with Superior Drop Test Performance

Dr. Weiping Liu and Dr. Ning-Cheng Lee

Indium Corporation of America

Fragility of SAC Solder Joints

- SAC solder joints are prone to crack at interface upon dropping, more profound for area array packages.
- Higher hardness than SnPb main cause.
- Reducing Ag helps, such as SAC105. But, still …
- A better LF alloy desired.

New Alloys Investigated

- SACX
  - SAC105 doped with small amount of elements
  - Some other doped SAC alloys
- Controls
  - Sn63
  - SAC105
  - SAC305
  - SAC387

Tests Conducted

- Melting Behavior
  - DSC, 2nd scan
- Drop Test
  - 10 samples for each condition
- Microstructure of cross-section and fracture surface
  - SEM/EDX
  - Optical Microscope
- Hardness
  - Vicker
- Creep

Schematic of test sample and drop tester setup

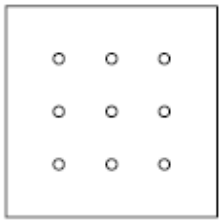

BGA coupon

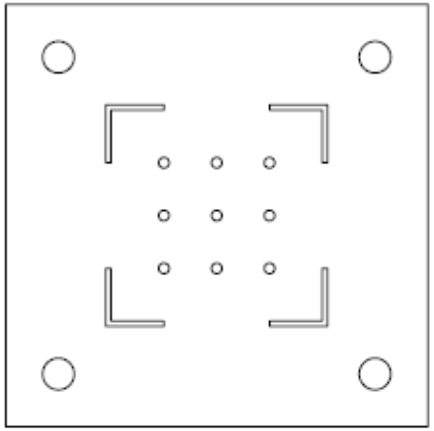

PCB substrate

BGA assembly

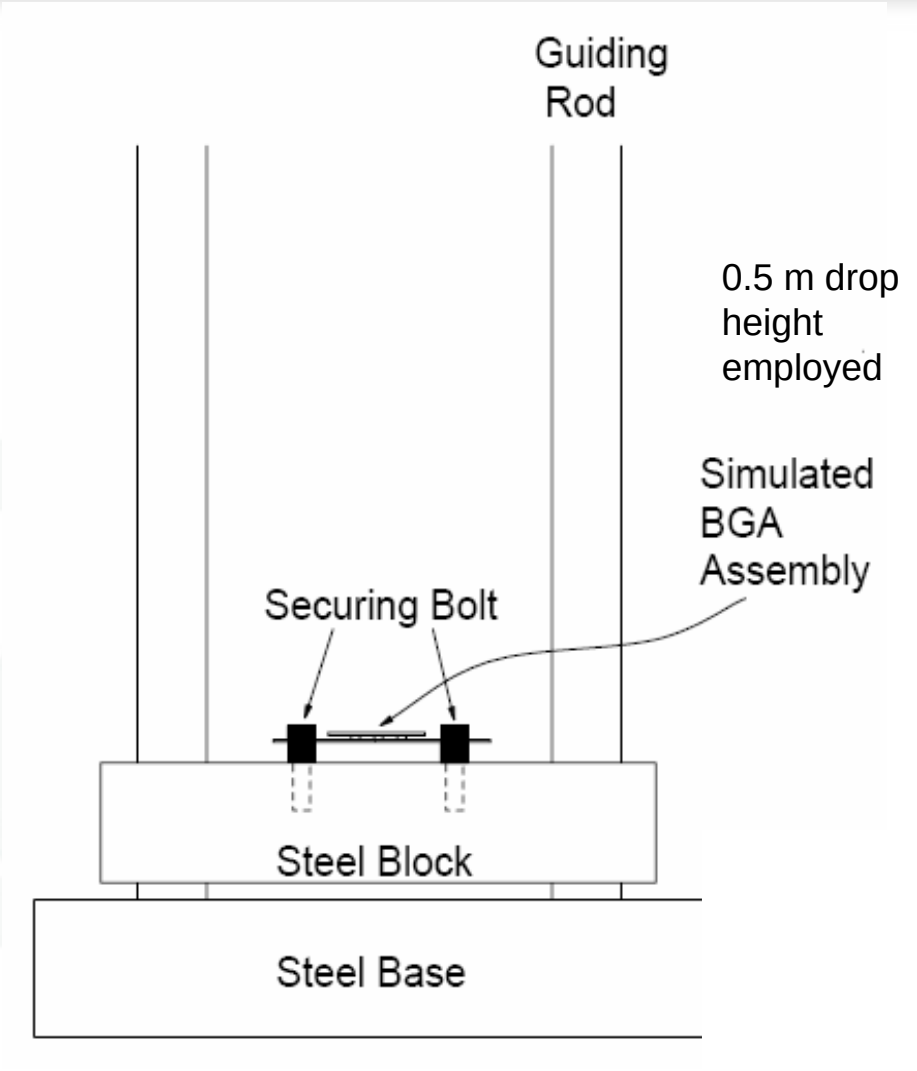

Melting behavior of solder alloys at the second scan of DSC analysis.

Alloys	Solidus (°C)	Liquidus (°C)
Sn1.1Ag0.64Cu0.13Mn	217.52	227.26
Sn1.13Ag0.6Cu0.16Mn	217.81	225.98
Sn1.07Ag0.58Cu0.037Ce	217.65	226.14
Sn1.0Ag0.46Cu0.3Bi0.1Mn	216.22	226.98
Sn1.05Ag0.73Cu0.067Ti	217.59	227.56
SAC105	217.18	226.8
SAC305	217.64	222.81
Sn63	180.75	183.72

DSC thermographs of second scan for Sn63, SAC305, SAC105, and Sn1.1Ag0.64Cu0.13Mn.

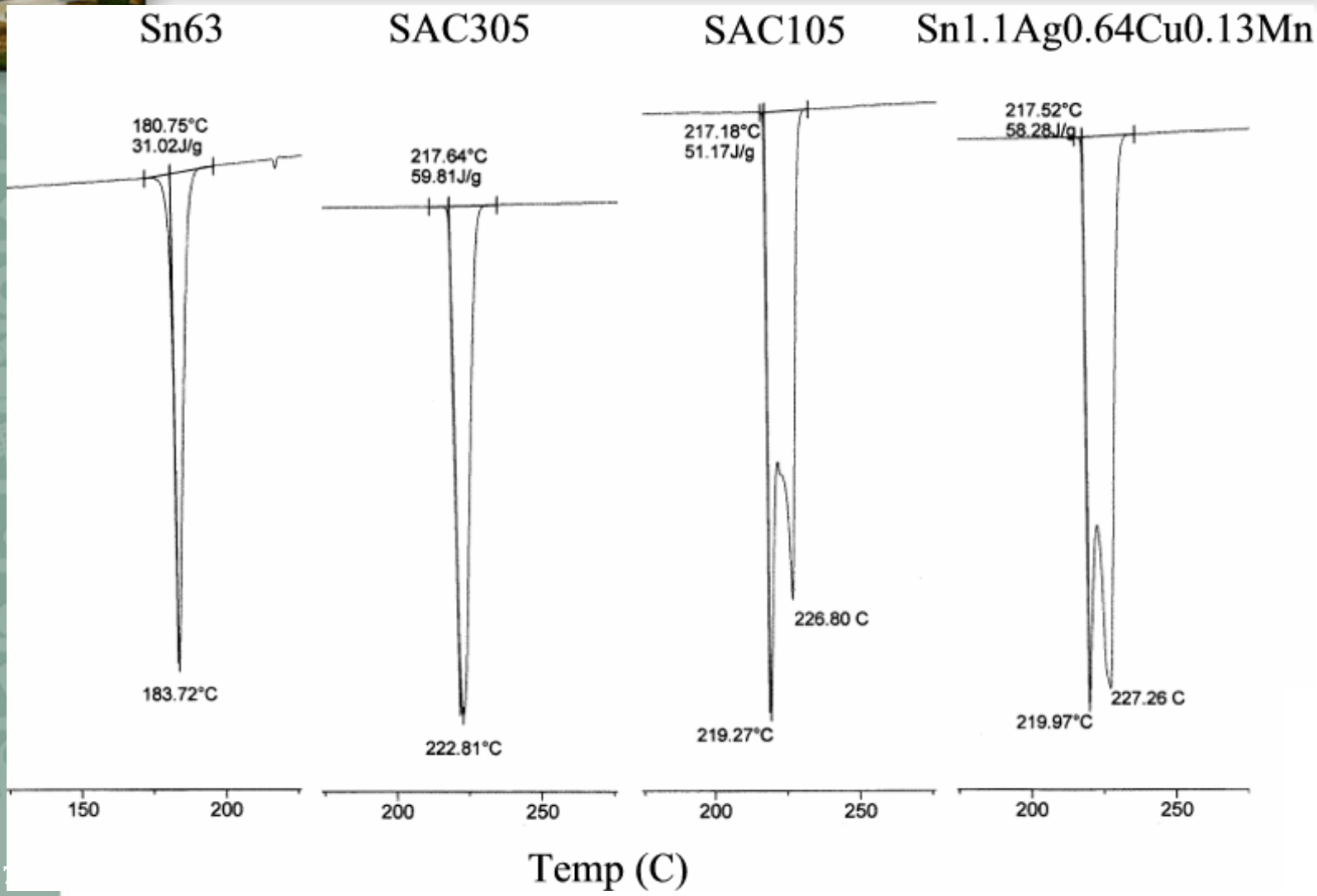

Drop test results of as-reflowed samples

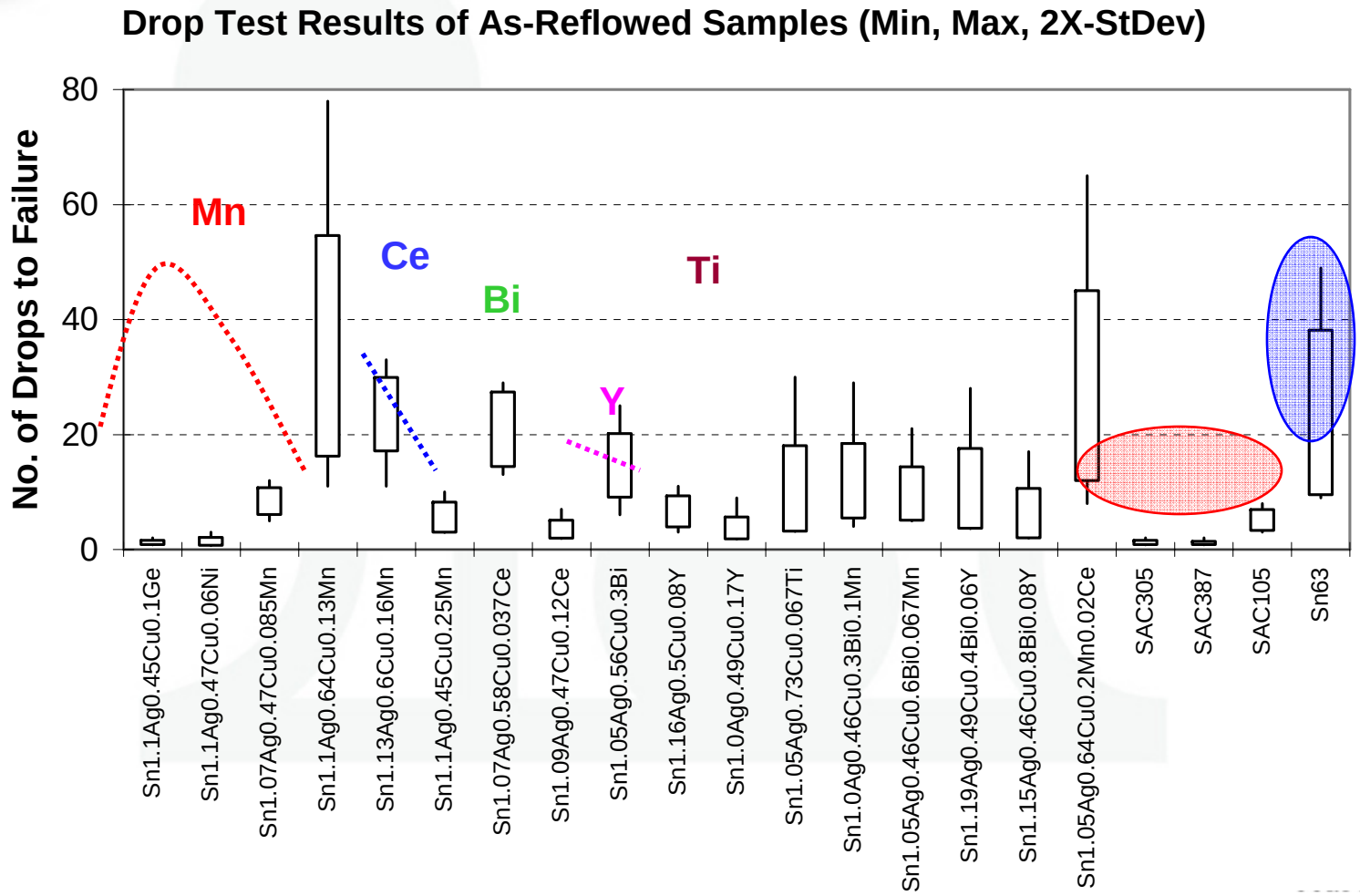

Mean values of drop test results for as-reflowed and after aging (150°C/4 weeks)

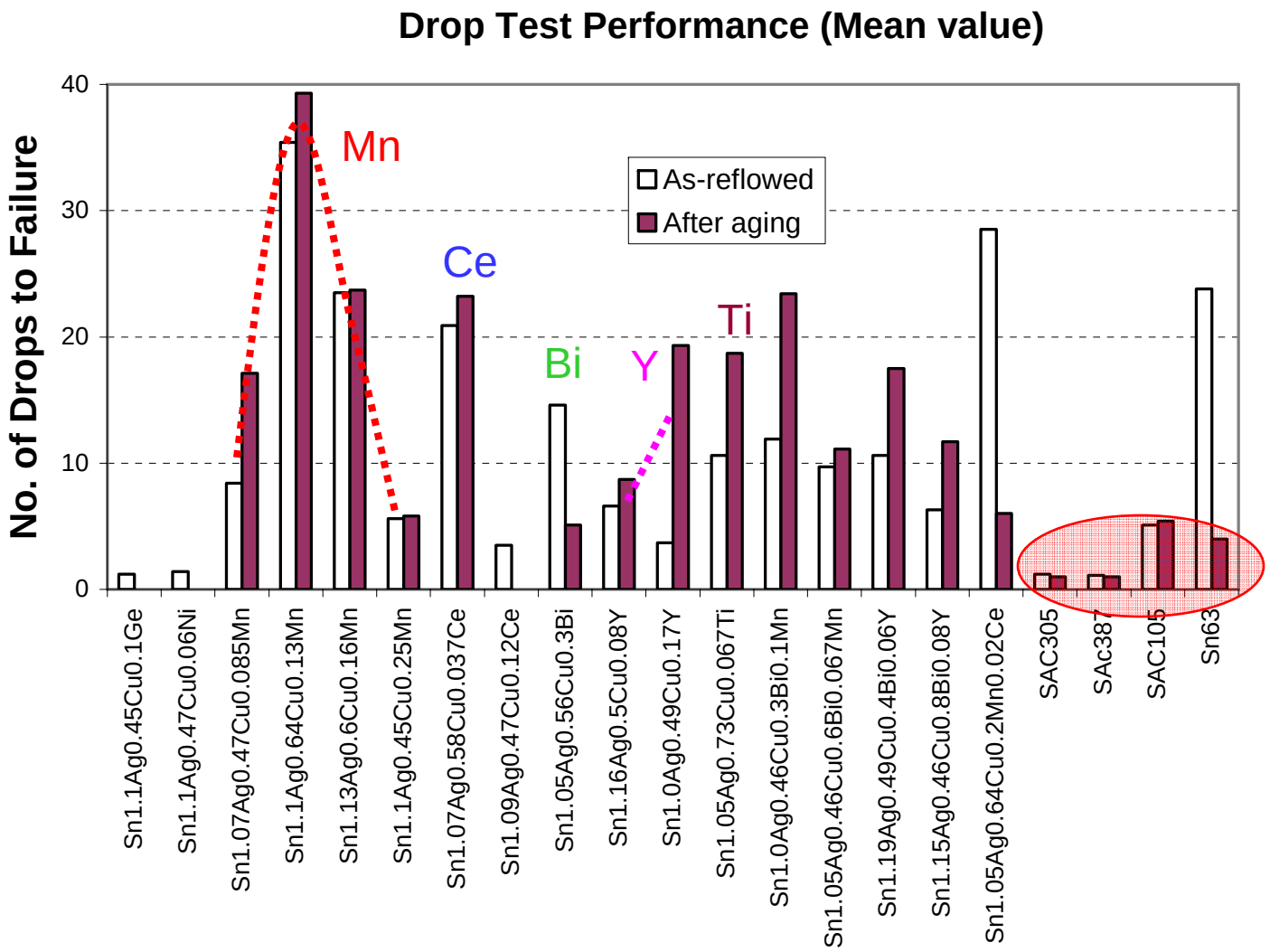

Effect of Ag content on drop test performance for as-reflowed samples.

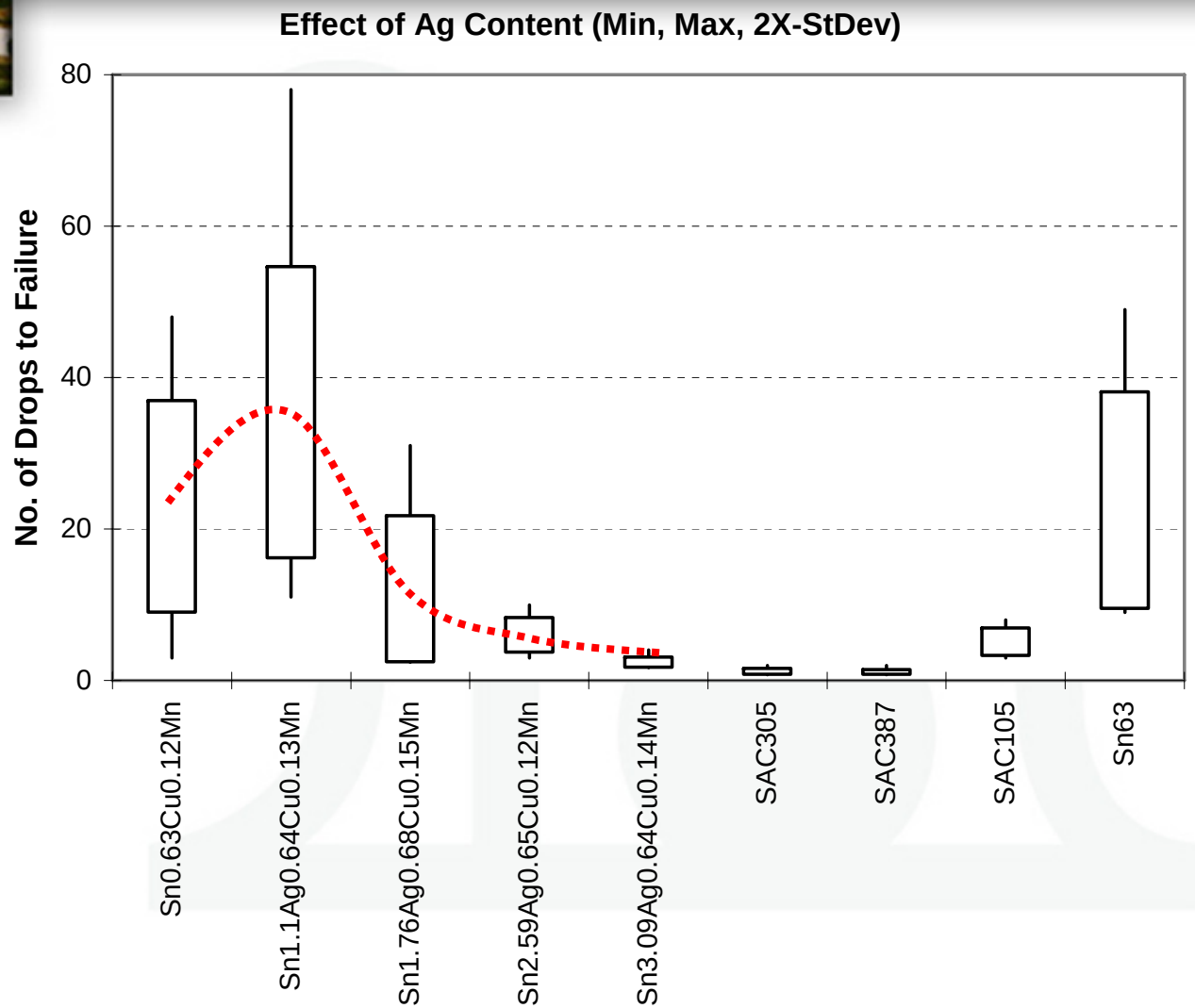

Fracture surface of drop test sample of SAC305.

For alloys with poor drop test performance, the fracture surface typically is flat, as exemplified by SAC305.

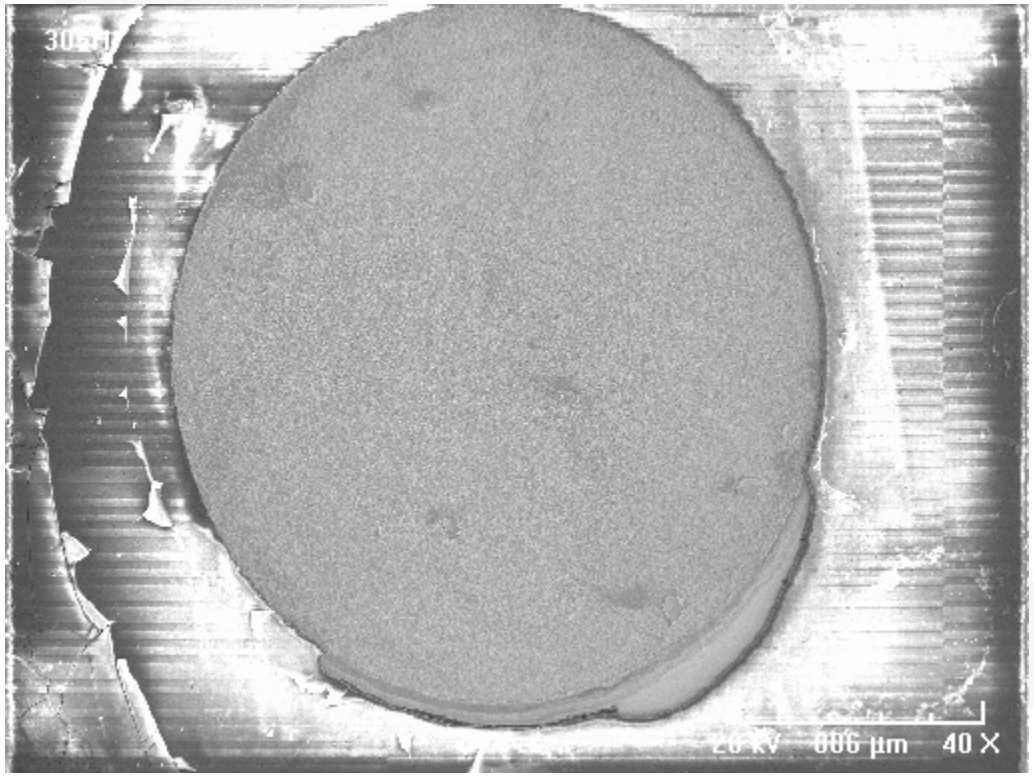

SEM image of fracture surface of drop test sample of SAC0.13Mn solder joint.

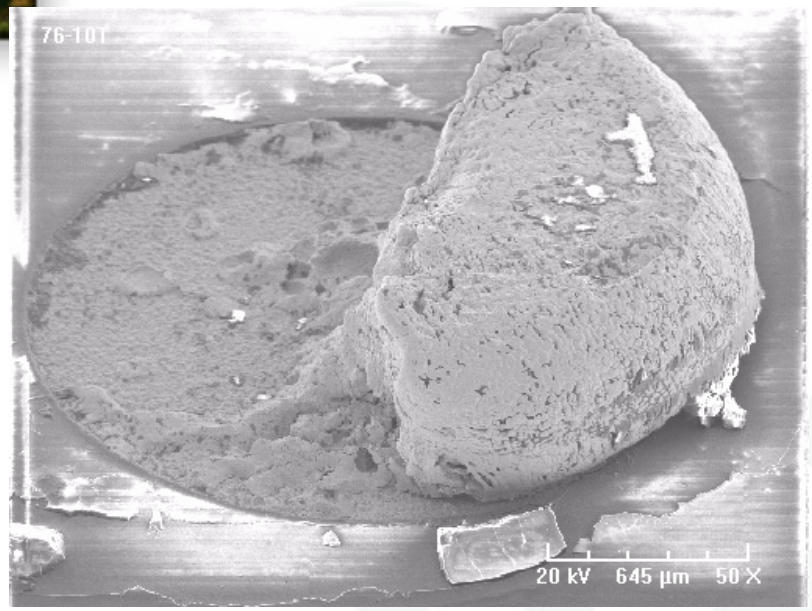

Solder observed at both side of fractured surface

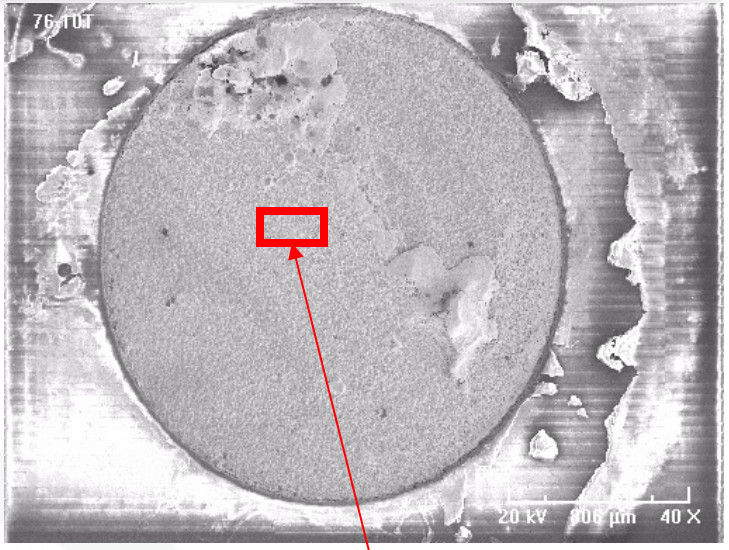

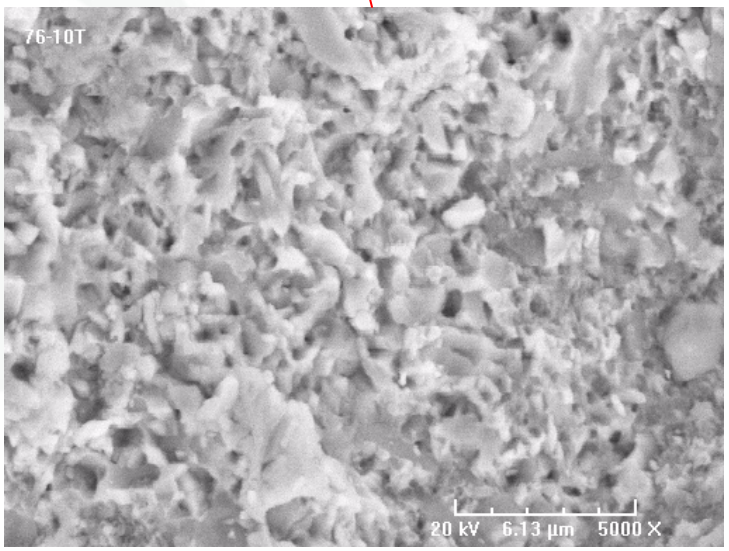

Effect of alloy on fracture pattern for as-reflowed drop test samples.

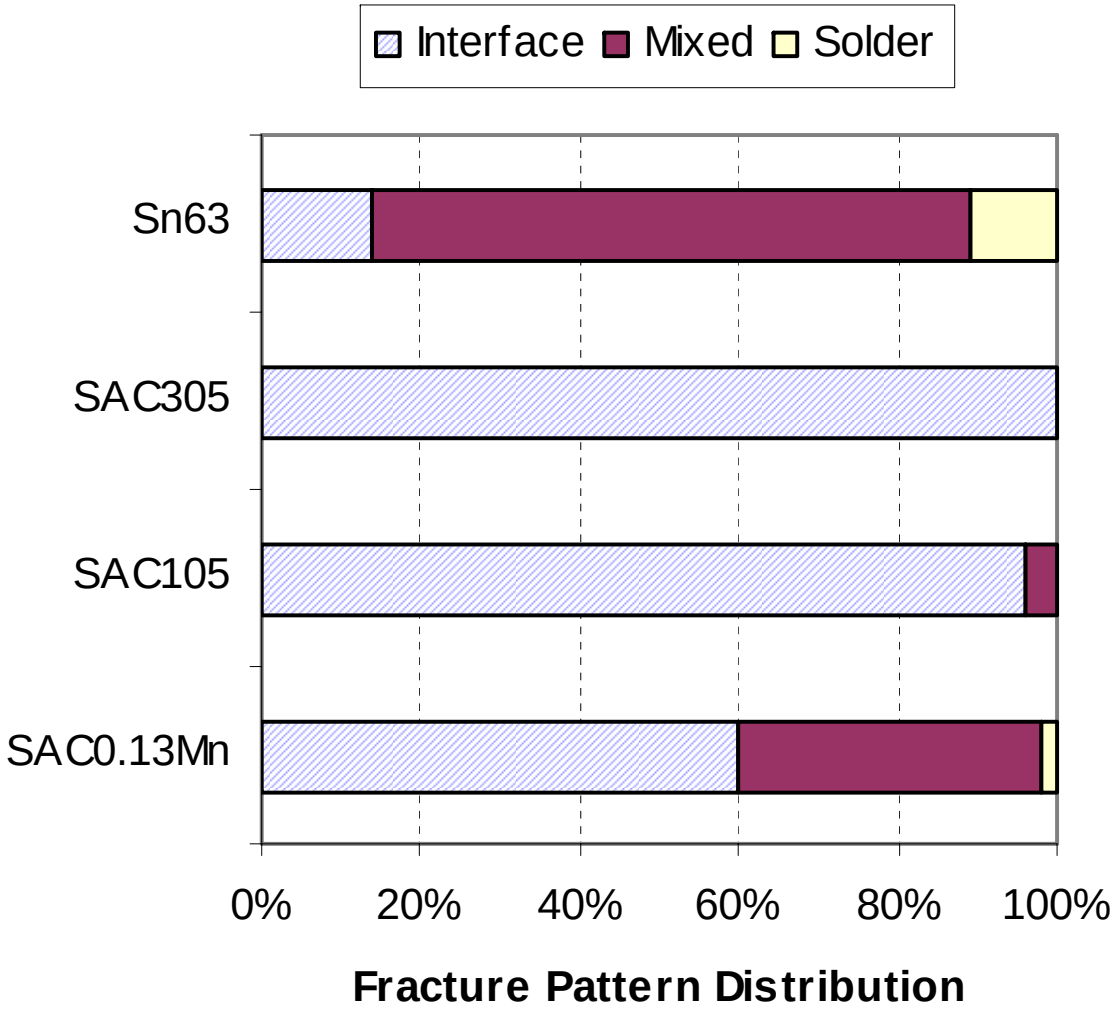

Drop test performance improves with increasing mixed mode and solder mode.

Ring Pattern common for high drop test performance joints

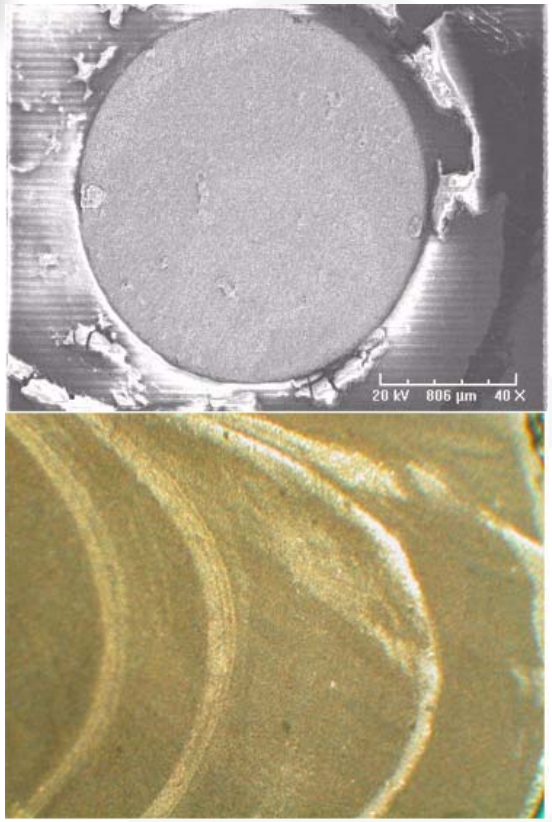

SEM image (top) of fracture surface of drop test sample of Sn1.1Ag0.45Cu0.25Mn and photo of fracture surface of Sn63 sample (bottom).

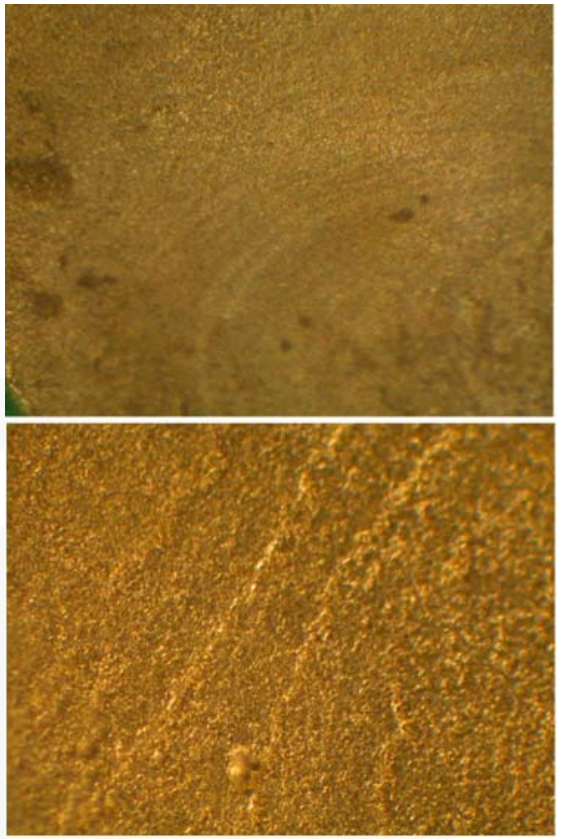

Ring pattern (top) on pads of drop test sample of Sn1.13Ag0.6Cu0.16Mn and close-up look (bottom) of the ring.

SEM image (100X) of cross-section of pads with ring pattern for fractured drop test sample of Sn1.05Ag0.56Cu0.3Bi

Here the convex shape of pad can be seen clearly, and is accompanied by a crack in the laminate layer underneath the pad. It appears that, upon drop test, the multiple bouncing of solder joint repeatedly lifted the pad, and the ring serves as water mark for the incremental fracture of solder joint.

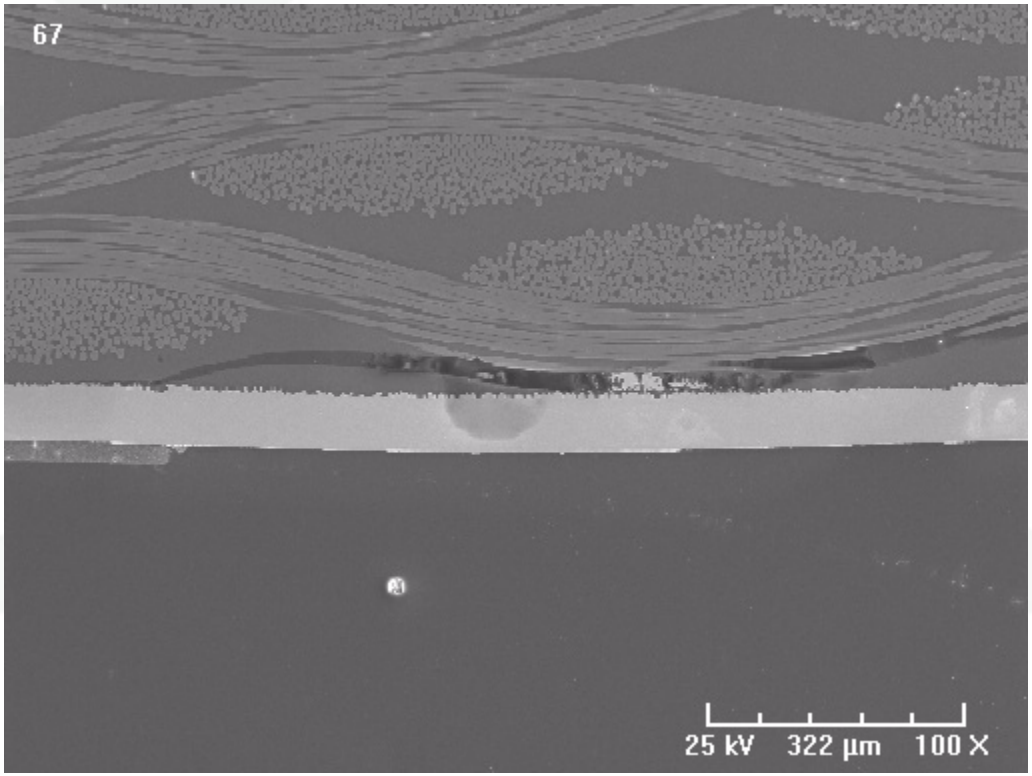

Elemental mapping (2000X) for open end of solder portion fractured at PCB pad side for drop test sample of SAC0.13Mn.

Mn is observed to cluster near intermetallics layer.

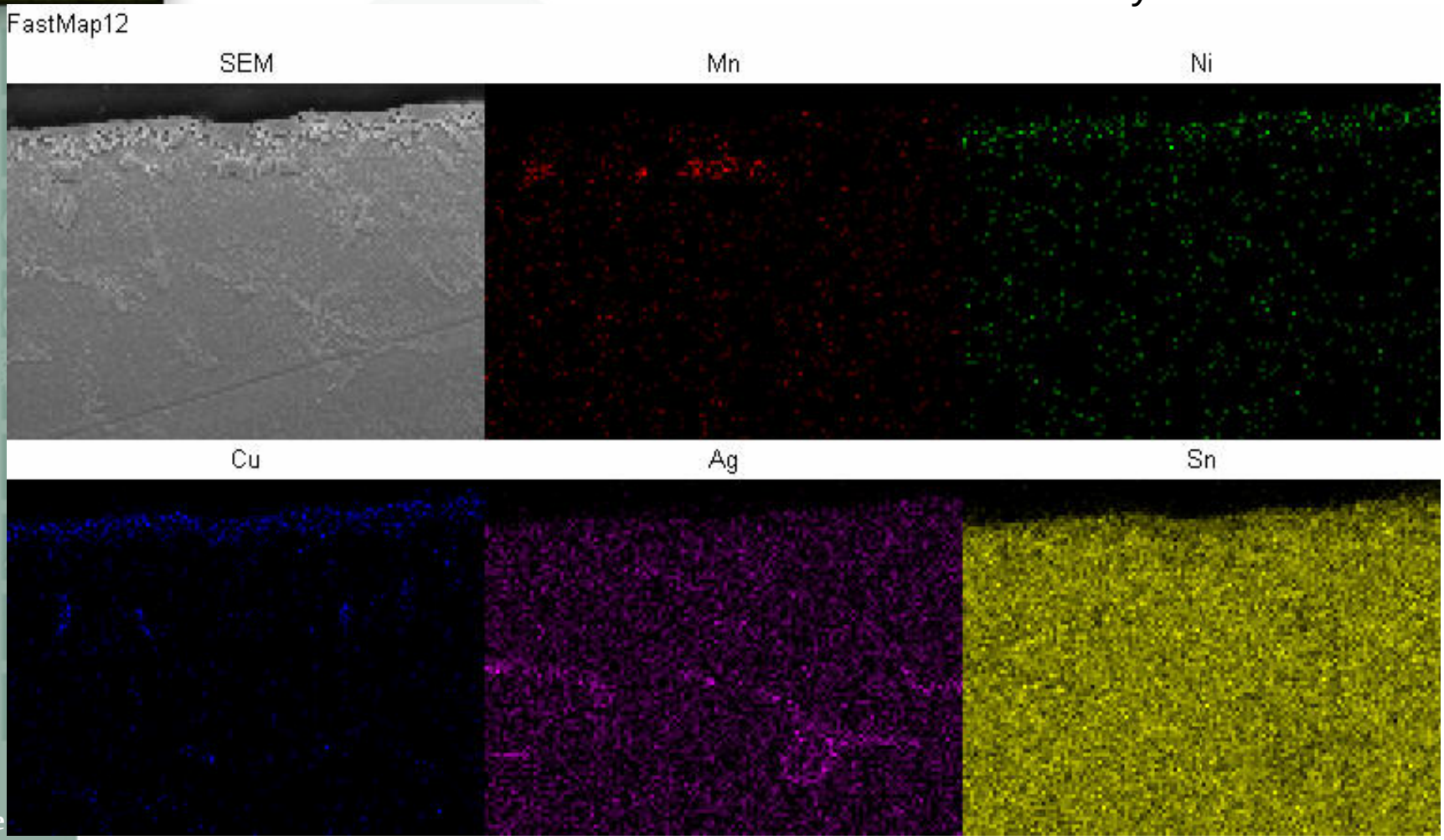

Elemental mapping (800X) for middle section of solder fractured at interface with PCB for drop test sample of SAC0.13Mn.

At location farther way from the intermetallics layer, such as the middle region of solder joint, no Mn can be discerned.

Furthermore, negligible amount of Mn can be detected near the BGA pad side. In this study, the solder bump was formed on PCB first, then followed by BGA coupon attachment. Mn appears to migrate toward PCB side during the first reflow, and scattered near the intermetallics layer. At the second reflow for BGA coupon attachment, the Mn seems to be unable to migrate back toward the BGA end in time to form an equilibrated distribution at both ends of solder joint.

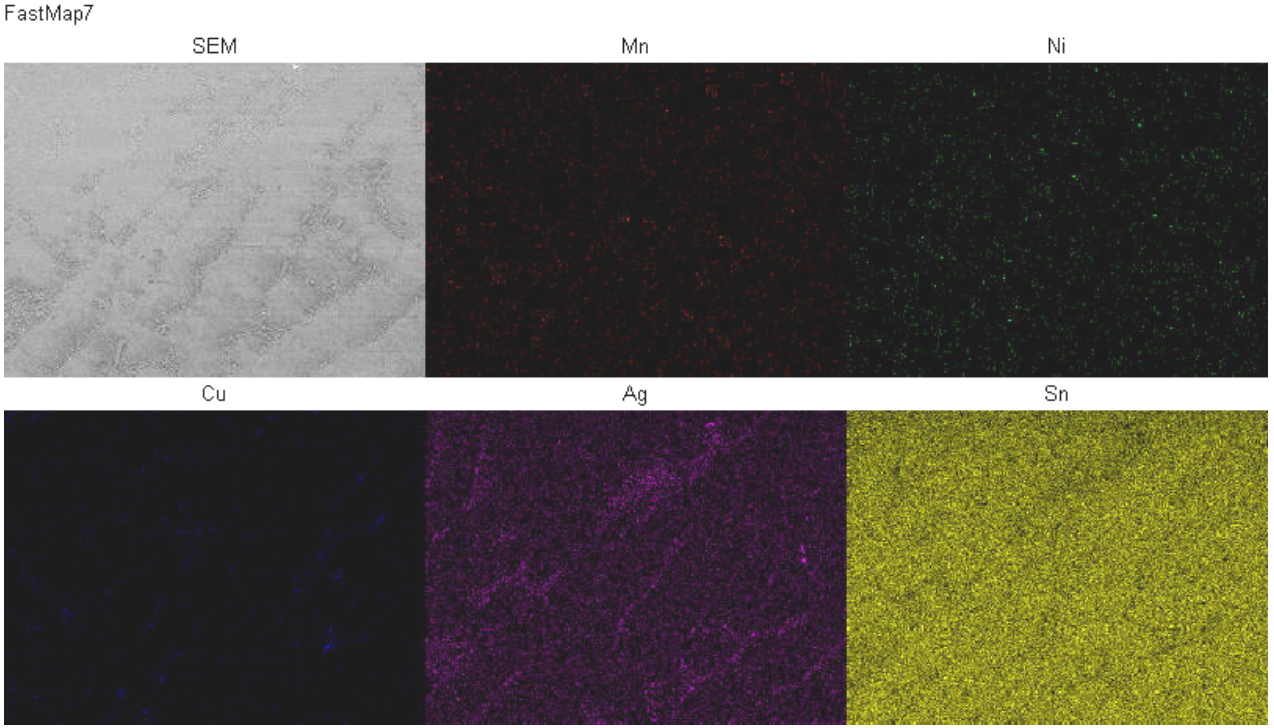

EDX elemental mapping (2000X) for drop test sample of SAC0.25Mn at interface of solder joint.

The form of Mn present in solder joint was studied by examining Sn1.1Ag0.45Cu0.25Mn (SAC0.25Mn), which exhibits a higher concentration of Mn than SAC0.13Mn, thus a greater sensitivity in analysis. The location of Mn is observed to be coincident with particulates, which are identified as MnSn2 intermetallics.

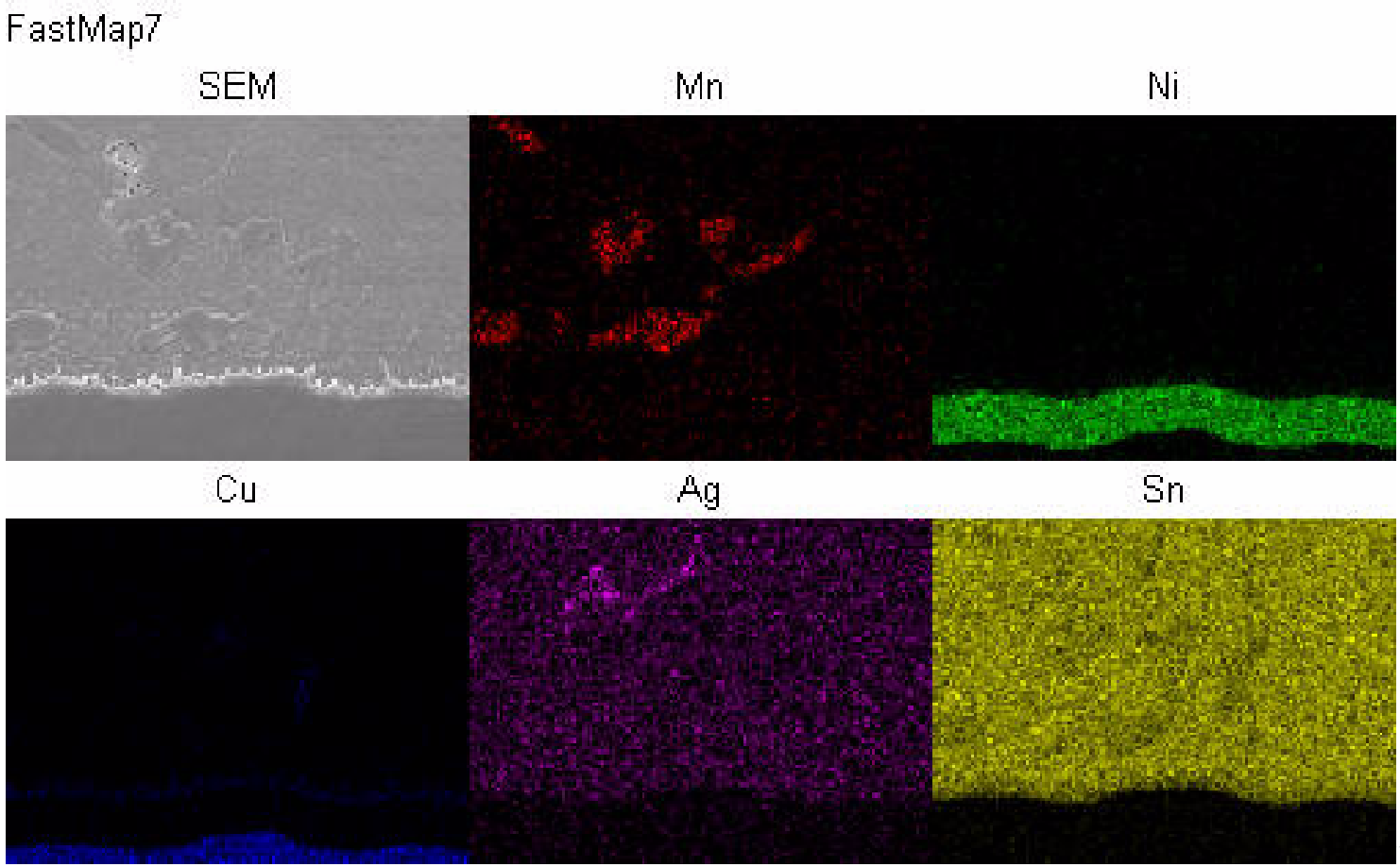

Relation between solder alloys and intermetallic compound thickness for as-reflowed and thermally aged condition.

All alloys except SAC387 exhibit an intermetallic compound (IMC) thickness around 0.9 µm for as-reflowed joints. This thickness roughly doubled after aging at 150°C for 4 weeks. By comparing as-reflowed drop test data with IMC data here, no correlation can be established between intermetallics thickness, intermetallics growth rate, and drop test performance.

Solder alloys	IMC (µm) As-reflowed	IMC (µm) Aged @150°C for 4 weeks
SAC0.13Mn	0.93	1.85
SAC0.16Mn	0.95	1.72
Sn63	0.86	2.04
SAC305	1.05	1.83
SAC387	1.4	2.5
SAC105	0.94	1.56

Hardness of solder alloys for as-reflowed samples.

Although the drop test performance appears to improve with decreasing hardness, this perceived relation suffers significant data scattering, suggesting the **bulk solder hardness is not a dictating factor**.

Alloy Composition	Hv (VHN) as-reflowed	Mean drop no. (as-reflowed)
Sn1.13Ag0.6Cu0.16Mn	12.6	23.5
Sn1.1Ag0.45Cu0.25Mn	12.9	5.6
Sn1.07Ag0.58Cu0.037Ce	13.1	20.9
Sn1.05Ag0.56Cu0.3Bi	14.6	14.6
Sn1.05Ag0.73Cu0.067Ti	13.2	10.6
SAC387	15.9	1.1
SAC105	12.9	5.1
Sn63	12.5	23.8

Creep test results of solder alloys determined at room temperature.

Majority of the SAC(X) alloys, including SAC0.13Mn, exhibit a lower creep rate than Sn63 at low stress condition. However, their creep rate increases rapidly with increasing stress, and at high stress condition, most of the SAC(X) show a higher creep rate.

A lower creep rate often suggests a longer fatigue life. In other words, at low stress condition, many of the SACX alloys not only exhibit a drop test performance better than SAC alloys or even better than Sn63, but very likely also exhibit a fatigue life better than Sn63.

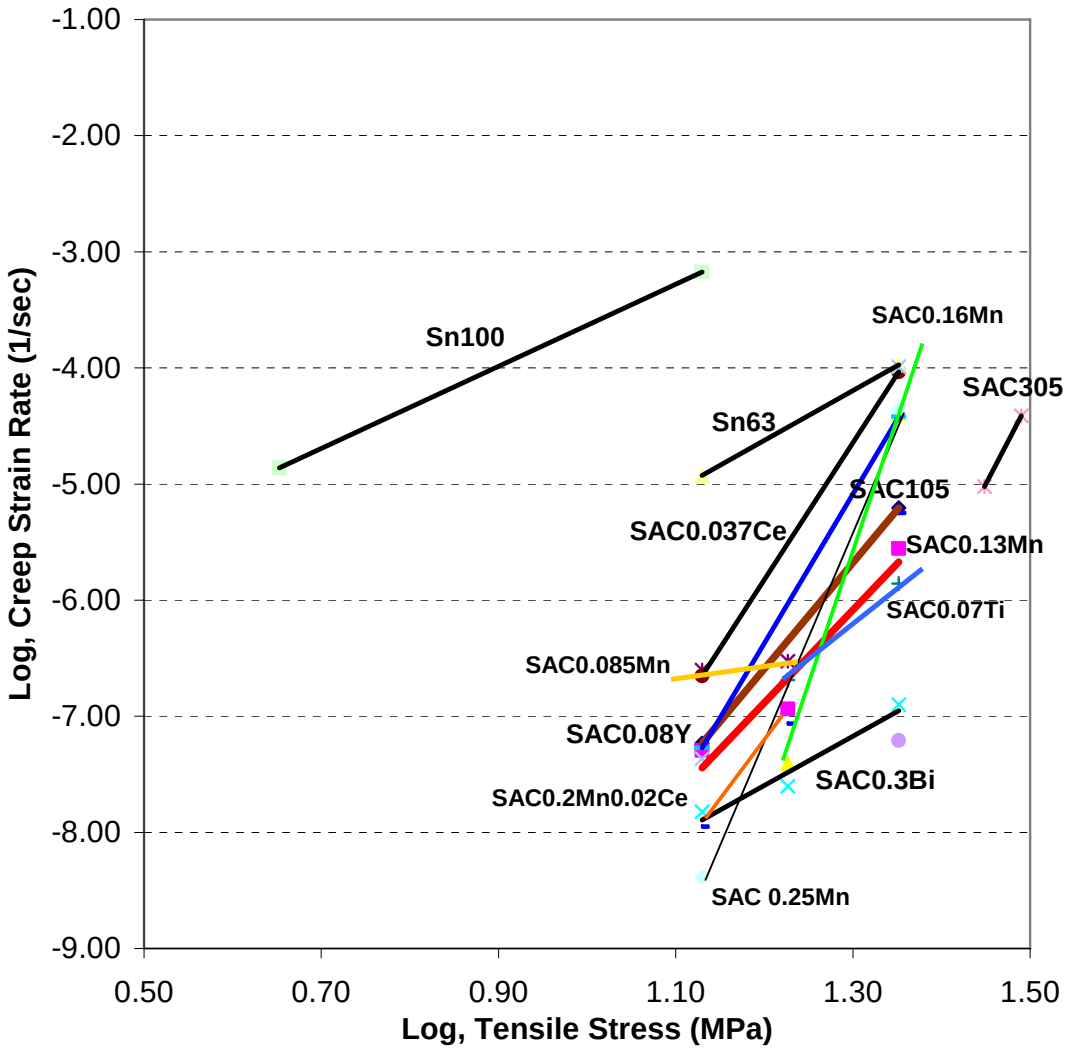

Discussion

- NiAu only used in this study.
- Clue of Mn role.
  - Mn not found in IMC layer, not affecting IMC thickness, growth rate & bulk hardness
  - MnSn2 particles tend to accumulate near IMC layer.
  - The fracture mode shifted from interface toward solder fracture, presumably caused by a reduced stress from solder exerted onto IMC layer.
- SACX alloys exhibit a better performance with thermal aging.
  - Could be due to softening of SACX solder due to consolidation of IMC particles during aging.
  - Or due to further migration of dopants toward IMC layer.

Conclusion

- Dopants Mn, Bi, Ti, Ce, and Y for SAC105 improve drop test performance when used alone or in combination, with Mn exhibiting the most profound effect.
- SAC+Mn outperformed not only SAC alloys, but also Sn63.
- Dopant not affecting melting, IMC composition, thickness, growth rate, and bulk solder hardness.
- $MnSn_2$ particles tends to migrate toward IMC and accumulate near IMC layer.
- At low stress condition, the lower creep rate of SACX than Sn63 suggests a lower fatigue rate.
- Thermal aging results in further improvement of drop test performance.

(Patent pending for novel materials presented in this work)

INDIUM CORPORATION